Machine Intelligence Research
www.mi-research.net

20(6), December 2023, 753-782
DOI: 10.1007/s11633-022-1364-x

Machine Learning in Lung Cancer Radiomics

Jiaqi Li[1] Zhuofeng Li[1] Lei Wei[1] Xuegong Zhang[1,2]

[1] Bioinformatics Division, Beijing National Research Center for Information Science and Technology (BNRIST) and Ministry of Education Key Laboratory of Bioinformatics, Department of Automation, Tsinghua University, Beijing 100084, China

[2] School of Medicine, Tsinghua University, Beijing 100084, China

Abstract: Lung cancer is the leading cause of cancer-related deaths worldwide. Medical imaging technologies such as computed tomography (CT) and positron emission tomography (PET) are routinely used for non-invasive lung cancer diagnosis. In clinical practice, physicians investigate the characteristics of tumors such as the size, shape and location from CT and PET images to make decisions. Recently, scientists have proposed various computational image features that can capture more information than that directly perceivable by human eyes, which promotes the rise of radiomics. Radiomics is a research field on the conversion of medical images into high-dimensional features with data-driven methods to help subsequent data mining for better clinical decision support. Radiomic analysis has four major steps: image preprocessing, tumor segmentation, feature extraction and clinical prediction. Machine learning, including the high-profile deep learning, facilitates the development and application of radiomic methods. Various radiomic methods have been proposed recently, such as the construction of radiomic signatures, tumor habitat analysis, cluster pattern characterization and end-to-end prediction of tumor properties. These methods have been applied in many studies aiming at lung cancer diagnosis, treatment and monitoring, shedding light on future non-invasive evaluations of the nodule malignancy, histological subtypes, genomic properties and treatment responses. In this review, we summarized and categorized the studies on the general workflow, methods for clinical prediction and clinical applications of machine learning in lung cancer radiomic studies, introduced some commonly-used software tools, and discussed the limitations of current methods and possible future directions.

Keywords: Machine learning, lung cancer, radiomics, medical image, clinical application.

Citation: J. Li, Z. Li, L. Wei, X. Zhang. Machine learning in lung cancer radiomics. *Machine Intelligence Research*, vol.20, no.6, pp.753–782, 2023. http://doi.org/10.1007/s11633-022-1364-x

1 Introduction

Lung cancer is the leading cause of cancer-related deaths in the world[1]. In 2020, there are around 2.2 million new cases of lung cancer with 1.8 million deaths worldwide[2]. The diagnosis, treatment and monitoring of lung cancer require accurate characterizations of tumors. Computed tomography (CT) is a standard non-invasive technology in clinic[3], providing information of the whole tumor in the form of images by representing heterogeneous cell populations and their spatial locations as various gray levels of pixels. In addition, positron emission tomography (PET) is often used along with CT as a functional imaging technology using agents such as ^{18}F-Fluorodeoxyglucose (^{18}F-FDG) to depict the activity of glucose metabolism[4]. In clinical practice, it is convenient and effective to visually examine the size, shape and location of tumors from CT and PET images[5].

In the past two decades, the growing interest in AI-based medical image analysis has generated a new area of research termed "radiomics". The term was first proposed by Lambin et al.[6] in 2012. It refers to the process that extracts mineable high-dimensional features from medical images. Radiomic studies have proposed multiple types of image features including qualitative semantic features, direct quantitative measurements that can be perceived by human eyes, and computation-based features that associate with the internal structure of a tumor[7]. These handcrafted features can capture both general properties and intra-tumor heterogeneity of tumors, which are often subsequently employed in machine learning models to predict tumor phenotypes, genotypes or patients' prognoses[8]. In recent years, deep learning showed its power in many pattern recognition tasks such as computer vision and natural language processing[9]. An important reason for such success is its great ability of feature extraction. Different from calculating predefined features, deep learning methods are able to continuously optimize model parameters during the training process to adjust feature extraction for better clinical predictions[10]. Deep learning extends radiomics from predefined features to a larger scope with abstractive features, delivering strong diagnostic information and prognostic efficacy[11].

This review first introduces the four consecutive steps of radiomic studies in lung cancer: image preprocessing, tumor segmentation, feature extraction, clinical predic-

Review
Manuscript received on May 13, 2022; accepted on August 6, 2022; published online on February 18, 2023
Recommended by Associate Editor Dao-Qiang Zhang
Colored figures are available in the online version at https://link.springer.com/journal/11633

tion (Fig. 1). Then, it summarizes recent studies focusing on the clinical prediction methods, their potential applications in lung cancer radiomics and some commonly-used software tools. Studies on this topic usually start with the preprocessing of chest CT or other modalities of images. Thresholding of pixel intensities with tissue-specific window sizes and levels is necessary for downstream analysis. If multiple image modalities are involved, image registration should be performed to align body structures across different modalities to the same coordinate system. For studies focusing on the tumor area, they are likely to perform segmentation to locate tumors for detailed analysis. Then, feature extraction is performed in which handcrafted or deep features are obtained as representations of images. After that, radiomic studies would specifically develop methods for clinical prediction using extracted features for different tasks. There are four main categories of clinical prediction methods: radiomic signature construction, tumor habitat analysis, cluster pattern characterization and end-to-end prediction of tumor properties. Tumor genotypes and phenotypes such as malignancy, histological subtypes as well as treatment outcomes are commonly used as the prediction targets.

The rest of this paper is organized as follows. Section 2 summarizes the general workflow of the radiomic analysis and common implementations in each step. Section 3 presents the four major categories of methods for clinical prediction. Section 4 reviews the clinical applications of radiomic studies on lung cancer in recent years. Section 5 introduces some commonly used software tools in the radiomic studies. Section 6 discusses the current challenges and highlights some future directions.

2 General workflow of radiomics

In general, it is difficult to make predictions of tumor properties directly from medical images. For example, a CT image consists of thousands of gray levels (Hounsfield units, HU), in which only a limited range of gray levels are lung tissues. Considering that some image noise may also exist, it would be misleading to extract features in original CT images for lung studies. Therefore, an image preprocessing step is necessary to filter out unrelated information from medical images. Also, cancer studies usually focus on the tumor and its surrounding area, which requires a tumor segmentation step prior to the following analysis. Next, we need to transform tumor images to mineable feature vectors through the feature extraction step. These steps make it feasible to design

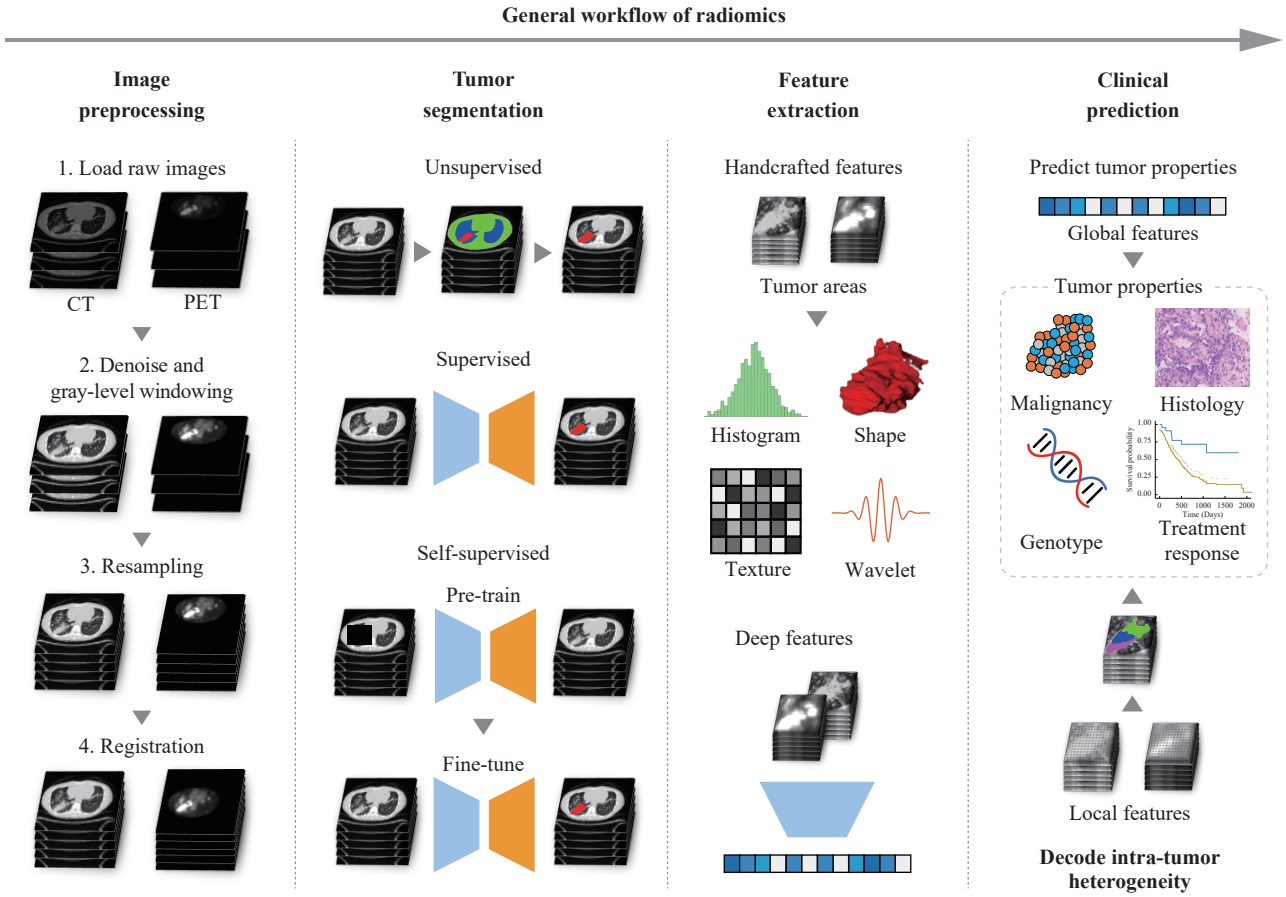

Fig. 1 Workflow of radiomics

methods for clinical predictions. In this section, we will follow the common workflow of radiomics (i.e., image preprocessing, tumor segmentation, feature extraction and clinical prediction) and summarize the current progress in each step. It is worth noting that the workflow also works for cancer types in addition to lung cancer. Fig. 1 provides an overview of the general workflow of radiomics.

2.1 Image preprocessing

It is necessary to conduct image preprocessing at the beginning of the analysis. The preprocessing step mainly contains denoising, gray-level windowing, resampling and registration between image modalities. First, noises can be introduced to medical images during the imaging process. Filtering and deep learning methods on both spatial and wavelet-transformed domains are designed to reduce noise and improve image quality[12]. Second, the spacing between pixels and the interval between slices (slice thickness) are often different among patients. Resampling should be performed to make the spacing uniform along three dimensions. Interpolation methods such as linear, cubic and nearest neighboring interpolations are often used in resampling[13]. Third, the original image contains a much larger HU range than that of lung tissues. If we directly scaled the HU value to the range from 0 to 1, the variation of lung tissue would be minimized to a small range, and important information would be missed for downstream analysis. Therefore, we should set a proper HU window size and level for specific tasks according to prior knowledge and only focus on image parts with HU values in this window. Finally, for multi-modality images like FDG PET/CT, each image modality is obtained separately. As a consequence, the relative position of body structures may be different in different image modalities. To better incorporate multi-modality radiomic information, image registration should be performed to align images with different modalities into the same coordination. Many registration methods have been proposed. For example, Mattes et al.[14] designed a strategy combining rigid body deformation and localized cubic B-splines to capture the motion between CT and PET images for further image alignment. Yu et al.[15] employed a deep learning model to learn a 3D non-rigid deformation for automatic image registration between PET and CT images. Image registration makes it convenient to transfer tumor segmentation and integrate radiomic information across image modalities.

2.2 Tumor segmentation

After the image preprocessing step, most studies would focus on the region of interest (ROI) for feature extraction. For lung cancer analysis, radiologists often contour the tumor region to obtain the segmentation masks manually, which is time-consuming. Also, the precision of segmentation highly depends on the experience of radiologists and sometimes can be subjective. With the development of machine learning, many algorithms have been designed to automatically obtain segmentation from medical images[16–18]. According to whether manual segmentation is included as the training target, these methods can be divided into three categories: unsupervised, supervised and self-supervised tumor segmentation.

Unsupervised segmentation methods

The unsupervised tumor segmentation adopts digital image processing methods such as thresholding, edge detection, region growth, and clustering. To reduce the influence of tumor-irrelevant parts, a two-step segmentation is often used, which first obtains the lung area and then finds tumors within the lung. Thresholding methods divide pixels into several levels according to their intensities[19]. Region growth methods set initial seed pixels and then expand each seed pixel by merging similar neighboring pixels to obtain the tumor area[20]. Clustering methods employ clustering algorithms like k-means to group pixels into several clusters. The pixel group with the highest intensity is more likely to be a tumor[21]. The unsupervised methods take a step forward to automatic tumor segmentation while the performances are limited, as other parts in lungs (e.g., vessels) may have similar intensities as tumors and can affect the segmentation results. Also, the judgment of candidate nodules/tumors still highly relies on human efforts.

Supervised segmentation methods

Supervised tumor segmentation methods usually take advantage of deep learning to better extract tumor-related radiomic information from medial images. Pixel-level delineation of the tumor area is used as the ground truth for model training. The deep learning model predicts whether each pixel in the image belongs to the tumor or the background, and the training process minimizes the difference between the predicted pixel labels and the ground truth. Supervised object segmentation models such as fully convolutional neural network (FCN)[22] and mask R-CNN[23] achieved great success in natural images. Besides the direct applications of these models on medical images, Ronneberger et al.[24] proposed U-Net, which is specifically designed for biomedical images. U-Net is composed of an encoder, a decoder and skip-connections between layers, which can capture multi-level radiomic information. U-Net processes 2D images, while the 3D U-Net model is proposed to better process image volumes[25]. The automated machine learning (AutoML) techniques are also used to improve U-Net performance by searching for the optimal parameters of neural networks[26]. There are also many architectures different from U-Net developed for tumor segmentation from medical images[11]. These models provide assistance for clinical use and shed light on the possibility of automatic tumor segmentation in the future.

Self-supervised segmentation methods

One important reason for the success of supervised tumor segmentation is the large number of labeled samples. However, it is common that many medical images remain in the picture archiving and communication system (PACS) of hospitals, while only a small number of them are manually delineated. It would be beneficial if those unlabeled data could be used to improve the model performance. Recently, self-supervised learning (SSL) has drawn increasing attention from researchers. The SSL strategy sets some proxy tasks to "pretrain" the deep learning model with unlabeled data, such as predicting rotation angles, solving jigsaw puzzles, contrastive learning, etc. In this way, the model is trained in a self-supervised manner. Then the pretrained deep learning model is fine-tuned using a small amount of labeled data. Experiment results show that the fine-tuned model is able to achieve comparable performance with fully supervised training if the SSL strategy is properly designed[27]. Several SSL methods have been proposed these years for the tumor segmentation tasks[28]. SSL provides a new perspective for automatic tumor segmentation in the condition of large datasets with fewer labeled samples, which deserves further exploration.

2.3 Feature extraction

Image features are important to the development of clinical prediction methods and their downstream applications. How to extract useful features remains to be one of the most important topics for radiomic studies. Many image features have been used in the past few decades and can be categorized into handcrafted features and deep features according to whether the feature has an explicit definition.

Handcrafted features

Handcrafted features are defined by scientists to decipher certain properties of a tumor image. The handcrafted features can be further divided into semantic features that are descriptive classification or grading of the tumor, and quantitative features that are continuous measurements and defined by mathematical formulas. The quantitative features are usually referred to as radiomic features in many studies.

Semantic features are the qualitative description of tumor size, shape and internal structures, which are usually perceivable by human eyes. They provide the presence or the level of some commonly used tumor properties, such as tumor roundness, spiculation, and air bronchogram. Experiment results show that semantic features can be applied to predict tumor genotypes[29]. Semantic features provide a preliminary method to characterize tumors from medical images, which facilitate the development of radiomics. However, the determination of semantic features is subjective and depends on experienced radiologists. It is usually difficult to make comparisons among different studies due to the divergent definitions. Also, semantic features restrict the extent of tumor description to the observation made by human eyes. Mining the unperceivable information behind images is still needed.

Quantitative features are continuous measurements of tumor characteristics from different angles. These features can also capture tumor information that cannot be perceived by human eyes, delivering rich information of the tumor for subsequent analyses. According to the definition, quantitative features can be divided into four categories: first-order statistics, shape features, texture features and wavelet features. First-order statistics are direct measurements of the image without transformation. These features describe the distribution pattern of pixel intensities such as the mean, maximum, quantiles, variation, etc., which are also named as "histogram" features. Shape features decipher the size and boundary characteristics of the ROI, which are independent from the pixel intensities and distributions. Examples of shape features are the perimeter, sphericity, maximum diameter, etc. The third category is texture features that quantify the internal structure of the ROI. The calculation of texture features relies on the intermediate count matrix which summarizes the local patterns on the image. Commonly used count matrixes include the gray-level co-occurrence matrix (GLCM), gray-level size zone matrix (GLSZM), gray-level run-length matrix (GLRLM), gray-level dependence matrix (GLDM) and neighboring gray-tone difference matrix (NGTDM). Each count matrix reflects a certain type of image characteristics, from which a set of texture features can be calculated. For example, GLCM summarizes the co-occurrence number of neighboring pixels with certain gray levels. When values concentrate to the diagonal on the GLCM, the corresponding image is relatively homogeneous. Examples of GLCM-based texture features are autocorrelation, contrast, cluster tendency, etc. Another category of quantitative features is wavelet features, which are first-order statistics and texture features extracted from the wavelet-transformed image. The transformation performs high-pass or low-pass filtering on each dimension of a 3D image, resulting in eight transformed images for feature extraction. Quantitative features are powerful in capturing tumor information from medical images. They are the most commonly used features in clinical applications with medical images. Aerts et al.[30] employed 440 predefined quantitative features and decoded tumor phenotypes and genotypes. Tomaszewski and Gillies[31] discussed the biological meaning of quantitative features. To make feature extraction more convenient, Griethuysen et al.[32] designed a Python package pyradiomics to calculate quantitative features with several lines of code, which has become a widely used tool for radiomic analysis.

Deep features

Different from handcrafted features with clear definitions, deep features are the general name for image fea-

tures extracted by deep neural networks. Most deep-learning-based radiomic studies employ convolutional neural networks (CNNs) to extract image features. Each layer of the CNN contains several convolutional kernels with a given size such as 5×5 and trainable parameters. Each kernel is shifted along the image, and a convolution operation is calculated between image intensities and kernel parameters to generate a feature map. Parameters for different convolutional kernels are different to capture multi-view image characteristics. In addition to convolution, the pooling operation is often used to merge neighboring pixels on the feature map to reduce feature dimensionalities. The maximum and average are two common pooling methods with a given size. In this way, CNN is able to capture basic features (boundary, corner points, etc.) in the first few layers, which are further integrated into higher-level features in the latter layers. After training, kernel parameters are optimized to extract useful information for the prediction goals and the flattened feature map of the last layer is regarded as the deep features of the image. Recently, a new deep learning model named vision transformer (ViT)[33] achieved superior performance in image analysis. ViT provides another approach for the extraction of deep features from medical images. It divides the image into several patches and obtains the vectorized embedding for each patch with a linear projection. Then, the patch embedding and corresponding position encodings are input to the transformer encoder. ViT takes advantage of the attention mechanism[34] and guides the model to focus more on the image parts related to the prediction goal[35]. There have been studies applying the ViT model to radiomic analysis for cancer[36].

2.4 Clinical prediction

The next step is clinical prediction using extracted features. People usually design methods to: 1) predict tumor properties or clinical outcomes such as nodule malignancy, tumor histologic subtypes and patient's prognosis or 2) obtain unperceivable tumor information and then correlate it with tumor properties or clinical outcomes. This is the most innovative part in the workflow of radiomics with many newly developed methods published in recent years. Besides algorithm design, evaluation is another important part to validate the effectiveness of the proposed methods. Scientists often collect patient cohorts from other institutes for external validation. The consistency of the evaluation performance across multiple institutes illustrates the robustness of the methods. The details of the methods for clinical prediction in radiomic analysis are introduced in Section 3.

3 Methods for clinical prediction

Radiomics is a research field with the rapid development of methods. We summarized current radiomic studies into four categories according to their methods for clinical prediction: radiomic signature construction, tumor habitat analysis, cluster pattern characterization and end-to-end prediction of tumor properties, which are illustrated in Fig. 2. Details of each category of methods and the comparison between them are described in this section.

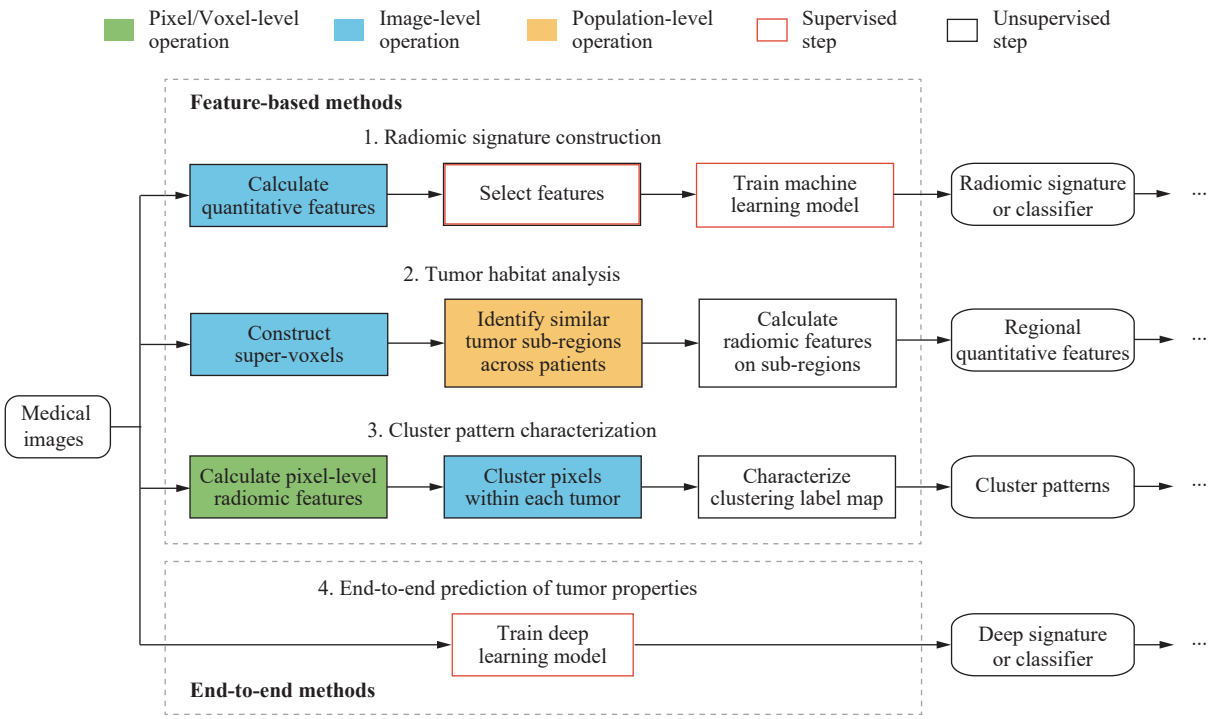

Fig. 2 Overview of clinical prediction methods in radiomic studies

3.1 Radiomic signature construction

The most commonly used method for radiomic analysis is building the radiomic signature, which is a continuous measurement of tumor characteristics and is potentially associated with certain clinical target(s). The calculation of a radiomic signature is the weighted sum of selected quantitative features introduced in Section 2.3:

$$Signature = w_1x_1 + w_2x_2 + \cdots + w_mx_m \tag{1}$$

where $\{x_1, \cdots, x_m\}$ are selected features and $\{w_1, \cdots, w_m\}$ are corresponding coefficients.

Feature selection

By definition, quantitative features usually contain many colinear features that do not provide additional information. Also, the high dimensionality of features would cause the overfitting problem in prediction[37]. Therefore, feature selection is important to build a meaningful and powerful radiomic signature. After selection, the remaining features are used to build the radiomic signature for clinical targets such as tumor histologic subtypes, patient′s survival conditions, etc.

The feature selection process usually includes feature stability assessment, correlation-based feature elimination and supervised feature elimination[30, 37]. The feature stability assessment includes the consistency evaluation of temporal, spatial and cross-dataset variations[37]. The assessment of temporal stability usually employs the "test-retest" setting, in which repeated CT scans (or other image modalities) on the same patient are performed with a time interval of several minutes. The assessment of spatial stability involves multiple delineations of the same tumor[30]. Quantitative features with high consistency between the test-retest CT images and different delineated areas of the same tumor are regarded as stable features for temporal and spatial stability, respectively. Similarly, radiomics features with high consistency between training and test datasets are considered as stable features[37]. Another feature selection step is correlation-based feature elimination, in which redundant features with high correlations between each other are identified. A correlation heatmap is often used to visualize feature correlations. It should be noted that the feature selection based on stability and correlation is unsupervised as no information of clinical targets is involved in this process.

The next step is supervised feature elimination with the involvement of clinical prediction target(s). There are three categories of supervised feature selection methods: filter, wrapper and embedded methods. Filter methods rank all the features using certain metrics (e.g., the correlation with the prediction target) and select top-ranked features to build radiomic signatures. Wrapper methods involve a prediction-selection loop to choose the most informative features. All features are used to make predictions, and a subset of features is selected iteratively according to the prediction performance of each feature. Embedded methods include feature selection in the classification algorithm. A common practice is adding a regularization term to the loss function. For example, the least absolute shrinkage and selection operator (LASSO)[38] method adds the sum of the absolute values of coefficients as a penalty:

$$\min_{w} \frac{1}{N} \sum_{i=1}^{N} \left(y_i - \boldsymbol{w}^{\mathrm{T}} \boldsymbol{x_i}\right)^2 + \lambda \|\boldsymbol{w}\|_1 \tag{2}$$

where N is the sample size, y is the prediction target, $\boldsymbol{w}$ is the coefficient vector, $\boldsymbol{x}$ is the selected feature vector and λ is the hyper-parameter that controls the proportion of penalty. LASSO regression minimizes the coefficients of irrelevant features down to zeros, and the features with non-zero coefficients are selected. By comparison with wrapper methods, embedded methods are computationally more efficient[39]. Different supervised feature selection methods are chosen according to the task. The classification tasks often adopt wrapper methods with support vector machine (SVM), such as R-SVM[40], SVM-RFE (recursive feature elimination)[41], etc. Regression tasks usually use embedded methods using LASSO regression. Specifically, for the prediction of patient′s survival time, people often choose the Cox proportional hazard (CPH) model to build the signature[42]:

$$h\left(t|\boldsymbol{x_i}\right) = h_0\left(t\right) \exp\left(\boldsymbol{w}^{\mathrm{T}} \boldsymbol{x_i}\right) \tag{3}$$

where $h\left(t|\,\boldsymbol{x_i}\right)$ is the expected hazard of sample $\boldsymbol{x_i}$ at time t, and $h_0\left(t\right)$ is the baseline hazard when all the features are equal to zero.

Signature construction and evaluation

After feature selection and parameter optimization, the radiomic signature is constructed and then applied to the test dataset to evaluate its effectiveness. If the obtained radiomic signature is highly consistent with the prediction target(s) on both the training and test datasets, it is considered to be an imaging biomarker that has the potential for clinical applications.

We have introduced the comprehensive steps of building a radiomic signature, but this does not mean that all the steps should be performed in clinical studies. Actually, studies in this direction follow a similar pipeline, but the detailed methods are designed specifically according to their research goals and datasets. For example, some studies directly make predictions using selected features without explicitly constructing radiomic signatures[43]. Feature stability assessment may not be performed due to the lack of test-retest CT images or multiple tumor delineations.

3.2 Tumor habitat analysis

Another category of methods is tumor habitat analys-

is. The name "habitat" comes from the tumorigenesis procedure. The uncontrolled growth of tumor cells leads to the independent promotion of local tumorigenesis, resulting in divergent local micro-environments[44, 45]. After natural selection on tumor cells, tumor sub-regions with similar environments would contain cells with similar genotypes and phenotypes[46]. These sub-regions become the "habitats" for a certain type of tumor cells[47]. As the genetic difference of cells affects the pixel intensity on medical images, people are able to partition pixels/voxels within the tumor area into several groups to identify the tumor habitats. Quantitative features can be calculated within each habitat to obtain the local characteristics of the tumor.

Multiparametric functional imaging is usually involved in tumor habitat analysis, such as ^{18}F-FDG PET/CT, hypoxia PET/CT (^{18}F-HX4 PET/CT) and dynamic contrast-enhanced CT (DCE-CT). These functional imaging modalities are designed to capture a variety of biological characteristics of the tumor, such as metabolic activity, hypoxia level, blood flow, etc., providing extra radiomic information for decoding intra-tumor heterogeneity. After image registration that aligns these functional imaging modalities to CT images, pixels/voxels are vectorized with clear biological meaning for each feature, which facilitates the habitat partition process.

According to the goal of habitat analysis, current studies on lung cancer can be divided into two types: identifying high-risk sub-regions or using local radiomic information to make more accurate predictions. Similar to the radiomic signature, clinical targets such as nodule malignancy, histological subtype and survival condition of patients are commonly used to evaluate the clinical value of these methods. The study by Wu et al.[48] is a pilot study for high-risk sub-region identification. The authors proposed a 2-step clustering process using FDG-PET and CT images. First, voxels in each tumor were merged into many "supervoxels" with k-means clustering. Next, they identified tumor sub-regions by grouping supervoxels via population-level hierarchical clustering. The volume of each sub-region was calculated and associated with patient's overall survival (OS) and out-of-field progression (OFP). The sub-region with the volume significantly associated with OS and OFP was regarded as high-risk. Even et al.[49] conducted a similar study. Besides CT and FDG-PET, HX4-PET images and images of blood flow (BF) and blood volume (BV) obtained from DCE-CT were also involved. They normalized each image modality and summed them into one merged image, then supervoxels were obtained with an adapted k-means clustering method named simple linear iterative clustering (SLIC)[50]. OS was also employed to identify high-risk sub-regions. Besides, the identified sub-regions can also be employed as mediators for the extraction of local quantitative features, which are further used to predict tumor malignancy[51] and histological subtypes[52]. Besides multiparametric functional imaging, Cherezov et al.[53] also explored the feasibility of solely using CT images to identify tumor sub-regions. The authors calculated wavelet features in patches of tumor images and then performed population-level clustering to group patches into sub-regions. Results showed that combining regional properties can better predict tumor malignancy.

All the studies employed supervoxels in habitat analysis, which aims to identify similar and neighboring pixels/voxels within the same tumor[48]. The supervoxel strategy is chosen to minimize the effect of registration uncertainties, reduce the amount of data and reduce noise[49]. Then population-level clustering is applied to group the supervoxels into sub-regions. Differences among these studies include the usage of functional imaging modalities, the method to construct supervoxels, and the metrics to determine the number of sub-regions. We summarized the characteristics of these studies in Table 1 and illustrated the common workflow in Fig. 3.

3.3 Cluster pattern characterization

The partitioning of tumor sub-regions in habitat analysis helps the extraction of local quantitative features. However, this category of studies does not consider the spatial distribution of tumor habitats, which is closely related to intra-tumor heterogeneity. Intra-tumor heterogeneity is an important issue in cancer studies as it may lead to drug resistance and therapy failure[54]. Intra-tumor heterogeneity is contributed by not only the diverse composition of cell populations but also their uneven distribution within the tumor. A comprehensive radiomic

Table 1 Summary of radiomic studies on tumor habitat analysis

Study	Goal	Image modality	Construction of supervoxels	Metric for sub-region number determination	Prediction target
Wu et al.[48]	Identify high-risk sub-regions	FDG PET/CT	k-means clustering	Gap statistics	OS of patients
Even et al.[49]		FDG PET/CT; HX4 PET/CT; DCE-CT	SLIC method	Calinski-Harabasz index	OS of patients
Chen et al.[51]	Extract local features for better predictions	FDG PET/CT	k-means clustering	Calinski-Harabasz index	Nodule malignancy
Shen et al.[52]		FDG PET/CT	k-means clustering	Calinski-Harabasz index	Histologic subtype
Cherezov et al.[53]		CT	Predefined patches	Gap statistics	Nodule malignancy

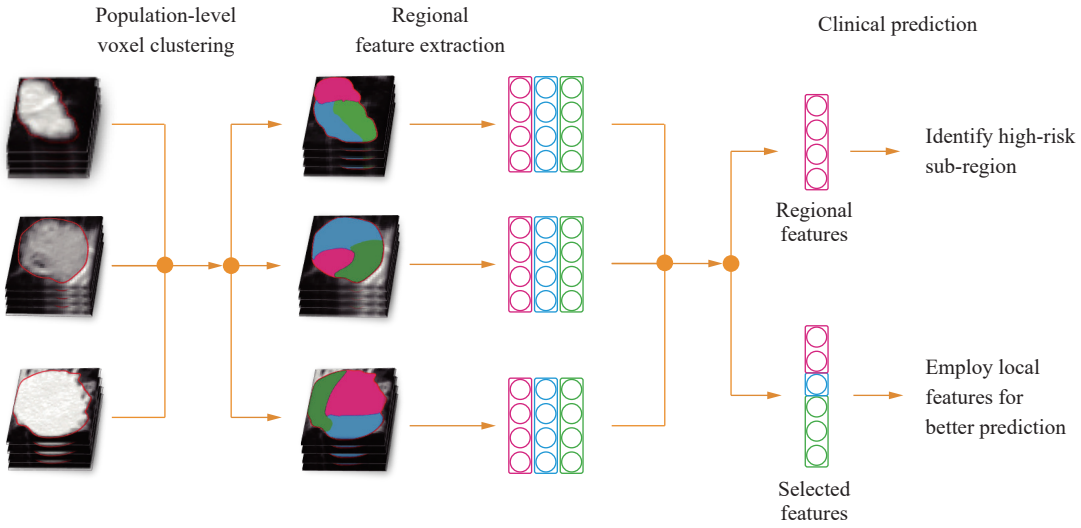

Fig. 3 Workflow of tumor habitat analysis

measurement of the tumor should also capture the distribution pattern of pixels/voxels on medical images.

To integrate both local and global information into the radiomic analysis, Li et al.[55] proposed a strategy named cluster patterns, which deciphers the distribution of similar sub-regions within the tumor. The cluster pattern is generated by the combination of local information extraction and global pixel clustering. First, the authors calculated quantitative features for each pixel from a squared window around it. Then, pixel clustering is performed to group tumor pixels into a fixed number of clusters. After coloring pixels with their clustering labels, the distribution pattern of similar sub-regions (i.e., cluster pattern) can be visualized. In a public patient cohort of lung cancer[30], they observed three cluster patterns, which were named as "unicore", "multicore" and "diffused", respectively. The unicore pattern is like concentric rings with a single centric region which implies weak heterogeneity, while the diffused pattern exhibits a scattered distribution with irregular shapes, indicating a higher heterogeneity level. The multicore pattern has multiple centric regions, which is in between unicore and diffused patterns. The cluster pattern provides an intuitive visualization and a mediator for measurements of intra-tumor heterogeneity, which was further illustrated by the close association with patient's survival conditions[55]. Fig.4 shows examples of CT images and calculated cluster patterns.

The cluster pattern categorization seems to be similar to the aforementioned habitat analysis, but they are different in many aspects. The partition of habitats requires the clustering of pixels or supervoxels across patients in the cohort, considering that the same type of tumor cells in different tumors would present similar radiomic characteristics on medical images. The generation of cluster patterns is performed in the same tumor without the usage of cross-tumor similarities, which is freed from the requirement of large patient cohorts. Another difference is the choice of cluster number. Instead of determining with metrics such as the Calinski-Harabasz index[56] or gap statistics[57], the cluster pattern characterization adopted multiple cluster numbers to observe the continuous change of cluster pattern, which further illustrates the degree of intra-tumor heterogeneity.

The cluster pattern study serves as a pilot study for a comprehensive description of intra-tumor heterogeneity in lung cancer. It is promising that the integration of multi-scale radiomic information could enhance the prediction for tumor phenotypes and patient's prognosis.

3.4 End-to-end prediction of tumor properties

Deep learning is a new category of methods used in radiomics these years[58]. According to the feature extraction mechanism introduced in Section 2.3, deep learning designs models in an end-to-end manner with medical images as the input and clinical targets as the output and optimizes model parameters for specific tasks. The optimization process is called a "training" process, in which the model tries to fit the data and labels guided by the loss function. The goal of training can be written in the following formula:

$$\min_{\boldsymbol{w}} Loss(f(x), y) \tag{4}$$

where x is the input data, y is the label, $f(\cdot)$ is the deep learning model, and $\boldsymbol{w}$ is the parameter set of $f(\cdot)$. The training process contains two parts: forward propagation and backward propagation[59]. In forward propagation, we input data into the model and calculate the values of nodes layer by layer to obtain the outputs $f(x)$. Then we compute the loss function and start back propagation, in which gradients of the loss function on each node are calculated from the output layer to the input layer. We

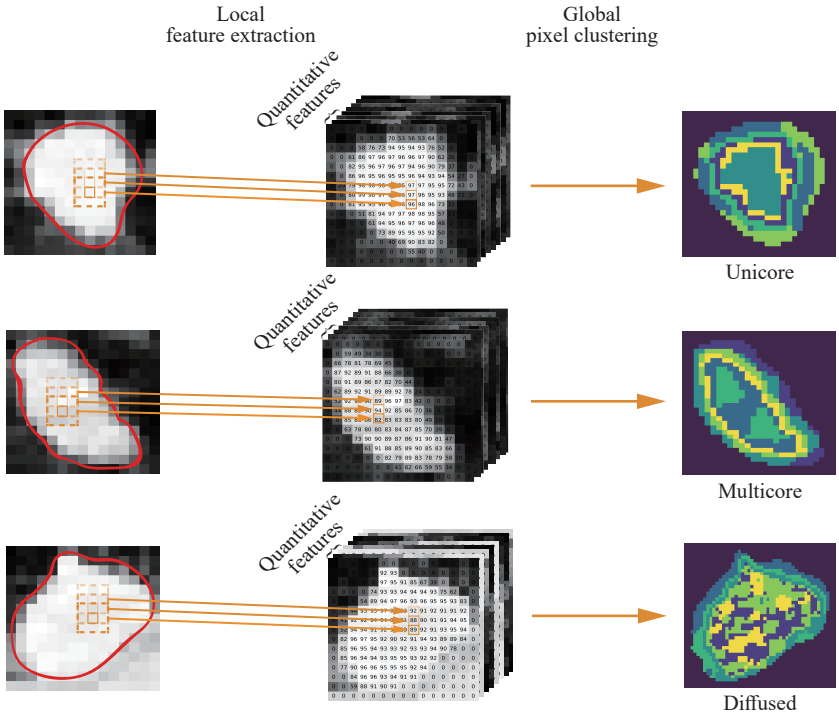

Fig. 4 Examples of CT images and calculated cluster patterns

update the parameters $\boldsymbol{w}$ using the preset learning rate ∂:

$$\boldsymbol{w_{i+1}} = \boldsymbol{w_i} - \partial \boldsymbol{\nabla} \tag{5}$$

where i is the number of training iterations, and $\boldsymbol{\nabla}$ is the gradients. The loss function is chosen according to the task. For example, cross entropy (CE) loss is used for classification tasks:

$$Loss\left(f\left(x\right), y\right) = -\sum_{c=1}^{M} y_{j,c} \log\left(f\left(x_j\right)_c\right) \tag{6}$$

where M is the total cluster number, $y_{j,c}$ is the binary label of sample j that belongs to cluster c, and $f\left(x_j\right)_c$ is the predicted probability of sample j that belongs to cluster c. For regression tasks, people often choose the mean square error (MSE) loss:

$$Loss\left(f\left(x\right), y\right) = \sum_{j=1}^{N} \left(f\left(x_j\right) - y_j\right)^2 \tag{7}$$

where N is the number of samples. In lung cancer studies, the survival time of patients is another research interest that is more than a regression task, as both the time length and the data censoring should be considered. The loss function for survival time prediction is designed according to the CPH model[42]:

$$Loss\left(f\left(x\right), y\right) = -\sum_{j \in U} \left(f\left(x_j\right) - \log \sum_{k \in F_j} \mathrm{e}^{f\left(x_k\right)}\right) \tag{8}$$

where U is the set of right-censored samples, F_j is the set of "at-risk" samples with event or follow-up times $F_j = \{k | Y_k \geq Y_j\}$, and Y_j is the event or last follow-up time of patient j[60].

Deep learning models usually rely on relatively large datasets to achieve good performance[61]. However, the annotation of medical imaging requires professional knowledge and experience, which is expensive and time-consuming. The number of medical image datasets is much less than that of natural images, such as ImageNet[62]. To solve the issue of data insufficiency, scientists employed the transfer learning strategy by using model parameters pretrained on ImageNet as initialization. Then the deep learning model is fine-tuned using lung cancer images and labels. The transfer learning strategy is widely used in lung cancer radiomics, such as predicting nodule malignancy[63] and treatment response[64].

3.5 Advantages and limitations

The four categories of methods introduced in this section have their pros and cons. The radiomic signature is easy to compute and interpret as each quantitative feature has a clear mathematical definition. But, these features are defined on the whole image and provide only global statistics. Although texture features count the frequency of local patterns (e.g., run-length of certain gray levels), they do not consider the distribution of the local patterns. The studies of habitat analysis focus more on regional properties without considering the global distribution of sub-regions. Besides, most habitat analysis studies involve multiparametric imaging modalities,

which may not be feasible for all clinical conditions. Loss of information, especially intra-tumor heterogeneity, exists in both radiomic signature and habitat analysis. The cluster-pattern-based method is proposed to solve this issue by integrating both local and global quantitative features, which provides a comprehensive characterization of the intra-tumor heterogeneity. The cluster pattern is built in an unsupervised manner so that the method possesses good generalization ability and there is no need for a large training dataset. But, it is required to choose proper parameters such as the cluster number to obtain meaningful cluster patterns. The end-to-end methods do not rely on predefined features but instead learn the feature extraction through supervised training. The integration of local and global features is also achieved. Recent end-to-end deep learning methods generally achieve better prediction performance than other methods in lung cancer studies. Compared with the non-deep-learning methods, the major limitations of deep learning are the interpretability and the requirement of a large amount of training data and computational resources[65]. It would be desirable that the advantages of different methods could be integrated to build more powerful radiomic methods in the future.

4 Clinical applications

Radiomics has the potential of broad applications in the diagnosis and treatment of lung cancer, in which the abovementioned radiomic methods play important roles in capturing unperceivable information from medical images to facilitate clinical decision-making. In this section, we discuss typical application scenarios such as the determination of nodule malignancy, histologic subtype classification, tumor genotype identification and treatment response prediction. It is worth noting that the reported performances may not be directly comparable among studies as the included patient cohorts are different.

4.1 Nodule malignancy classification

Lung cancer screening is widely used to help discover tumors at early stages to start treatment as soon as possible. One important step for lung cancer screening is to determine the malignancy of lung nodules, in which the biopsy is commonly used. However, the biopsy is invasive and time-consuming, which may not be suitable for the screening of lung cancer. Medical imaging tools like CT provide a chance to distinguish malignant and benign nodules non-invasively.

Both predefined handcrafted features and deep learning have been used for nodule classification. For example, Hawkins et al. downloaded CT scans of 196 patients from the national lung screening trial (NLST)[66] and extracted 219 quantitative features from 3D CT images. They performed feature selection to remove redundant and unstable features, leaving 23 features for classification. Then the authors tried multiple machine learning models such as decision tree, random forest, naïve Bayes and SVM to predict tumor malignancy using the selected features[67]. Similarly, Wu et al.[68] combined semantic and quantitative features from CT images and clinical factors of patients in a prediction model. Xie et al.[69] designed a knowledge-based deep learning model to address this problem. They took the 2D image sections from 9 different angles of the 3D CT image volume to obtain multiple views of the chest. For each view, the nodule segmentation mask was used to generate three knowledge-based nodule images, including the nodule and surrounding area, the peritumor area and the voxel heterogeneity

Table 2 Summary of radiomic studies on nodule malignancy classification

Study	Image modality	Dataset	Features	Reported performance
Hawkins et al.[67]	CT	196 patients (from NLST)	Quantitative features	AUC: 0.83 ACC: 0.80
Wu et al.[68]	CT	238 patients (in-house cohort)	Semantic features, quantitative features, clinical factors	AUC: 0.88
Wang et al.[70]	CT	593 patients (from LIDC-IDRI)	Quantitative features	ACC: 0.76
Beig et al.[71]	CT	290 patients (in-house cohort)	Quantitative features	AUC: 0.80
Xie et al.[69]	CT	1 018 patients (from LIDC-IDRI)	Deep features	AUC: 0.96 ACC: 0.92
Shen et al.[72]	CT	1 010 patients (from LIDC-IDRI)	Deep features	AUC: 0.93 ACC: 0.87
Zhang et al.[73]	FDG PET/CT	135 patients (in-house cohort)	Quantitative features	AUC: 0.89 ACC: 0.82
Chen et al.[74]	FDG PET/CT	149 patients (in-house cohort)	Quantitative features	ACC: 0.86
Kang et al.[75]	FDG PET/CT	268 patients (in-house cohort)	Quantitative features	AUC: 0.92
Park et al.[76]	FDG PET/CT	359 patients (in-house cohort)	Deep features	AUC: 0.84 ACC: 0.77

* We only recorded the reported performance on test or external validation cohorts. If multiple methods are used, the highest performance is recorded. The other tables are the same in this paper.
**The reported performances may not be directly comparable among studies as the included patient cohorts are different.

map, which were then input into a CNN model. The output vector of all knowledge-based nodule images from all 9 views was concatenated to predict the malignancy of nodules[69]. These studies used the lung image database consortium and image database resource initiative (LIDC-IDRI) dataset, which contains CT images paired with nodule position information of 1 010 patients. We summarized typical studies on nodule malignancy classification in Table 2.

4.2 Histologic subtype identification

There are two major types of lung cancers – Non-small cell lung cancer (NSCLC) and small cell lung cancer (SCLC). Approximately 85% of lung cancers belong to NSCLC and the other 15% belong to SCLC. NSCLC can be further divided into three major histologic subtypes: adenocarcinoma (ADC), squamous cell carcinoma (SCC), and large-cell carcinoma (LCC)[77]. There is also a small proportion of lung cancers not belonging to any of the three subtypes, which are named as "not otherwise specified (NOS)". As the treatment efficacy of lung cancer highly depends on the histologic subtype[78, 79], identification of the cancer subtype is an important step in the diagnosis of lung cancer.

With the development of imaging technologies, scientists have tried to explore the possibility of identifying histologic subtypes from a radiomic perspective. For example, Wu et al.[80] selected a subset of non-redundant features that correlate with histology from 440 predefined quantitative features, and then built machine learning models including random forest, naïve Bayes and k-nearest neighbors to classify ADC and SCC using the selected features. Similar studies have been conducted with different patient cohorts, quantitative features and methods[81, 82]. Besides CT, FDG PET imaging is often used to provide additional radiomic information[83–85]. There are also studies using deep learning for the classification task. Chaunzwa et al.[86] employed the transfer learning strategy to fine-tune the VGG-16 model with parameters pretrained on ImageNet. Marentakis et al.[87] tried several classical CNN architectures (e.g., AlexNet, Inception, ResNet) for feature extraction of each image slice and designed a long-short-term memory (LSTM) model to integrate radiomic information among slices. Guo et al.[88] performed the analysis in a different manner by directly training a self-designed 3D CNN model for the classification task. The relevant studies are summarized in Table 3.

In recent years, scientists have further proposed subtyping methods for NSCLC subtypes, such as ADC. The progression of early-stage lung ADC usually undergoes several stages: adenocarcinoma in situ (AIS), minimally invasive adenocarcinoma (MIA) and invasive adenocarcinoma (IAC)[92]. The phenotype and prognosis of the tumor highly depend on the histology stage. For example, the cure rate for tumors in AIS and MIA stages is nearly 100%, while it decreases substantially for IAC[93]. Radiomic approaches are used for the identification of these lung ADC subtypes[94, 95]. People can also classify tumors into earlier or later stages to judge their invasiveness (AIS VS. MIA/IAC)[96] or malignancy (AIS/MIA VS. IAC)[97–102].

4.3 Radiogenomics

Tumorigenesis and tumor progression are complex biological processes that involve complicated gene mutations and interactions. Tumorigenesis usually starts from the alteration of genes responsible for the reproduction,

Table 3 Summary of radiomic studies on histologic subtype classification

Study	Classification task	Image modality	Features	Reported performance
Wu et al. [80]	ADC VS. SCC	CT	Quantitative features	AUC: 0.72
Zhu et al.[81]	ADC VS. SCC	CT	Quantitative features	AUC: 0.89
Bashir et al.[82]	ADC VS. SCC	CT	Semantic features	AUC: 0.82
			Quantitative features	AUC: 0.50
Sha et al.[83]	ADC VS. SCC	FDG PET/CT	Quantitative features	AUC: 0.78
Hyun et al.[84]	ADC VS. SCC	FDG PET/CT	Quantitative features	AUC: 0.86
Koyasu et al.[85]	ADC VS. SCC	FDG PET/CT	Quantitative features	AUC: 0.84
Chaunzwa[86]	ADC VS. SCC	CT	Deep features (CNN)	AUC: 0.71
Marentakis et al.[87]	ADC VS. SCC	CT	Deep features (LSTM+CNN)	AUC: 0.78
Ubaldi et al.[89]	ADC VS. SCC VS. LCC	CT	Quantitative features	AUC: 0.72
Guo et al.[88]	ADC VS. SCC VS. SCLC	CT	Deep features (CNN)	AUC: 0.84
Liu et al.[90]	ADC VS. SCC VS. LCC VS. NOS	CT	Quantitative features	ACC: 0.86
Patil et al.[91]	ADC VS. SCC VS. LCC VS. NOS	CT	Quantitative features	ACC: 0.88

*The reported performances may not be directly comparable among studies as the included patient cohorts are different.

survival and differentiation of cells, which further activates or suppresses the expression of downstream genes in certain biological pathways and results in uncontrolled cell growth[103]. It is important to identify changes in cancer-related genes and pathways to individualize treatment plans for patients, which is the goal of precision medicine[104]. Traditional genomic analysis relies on tissue-based assays using biopsy or surgery. However, these methods rely on invasive sampling, which is harmful to the human body and cannot be applied to all clinical scenarios[105]. Furthermore, lung cancer presents strong intra-tumor heterogeneity with diverse composition and spatial distribution of cells within the same tumor[106]. The genotype of the sampled region may be different from the other parts of the tumor. Insufficient information of intra-tumor heterogeneity probably results in drug resistance and therapy failure, which is a major impediment to cancer treatment and prognosis[107]. Therefore, people are exploring the possibility of comprehensively decoding tumor genotypes from medical images, which facilitates the development of radiogenomics.

Radiomics and gene mutations

In lung cancer, many radiogenomic studies focus on the prediction of gene mutations from CT images. Mutation detection of some cancer-related genes such as epidermal growth factor receptor (EGFR), anaplastic lymphoma kinase (ALK), Kirsten rat sarcoma virus (KRAS) and serine/threonine-protein kinase B-Raf (BRAF) has been widely used for treatment selections[108]. The development of drugs targeting these genes significantly improves the treatment effects and prognosis of patients[109]. Accurate and efficient prediction of gene mutations from CT images would greatly benefit the precision medicine in lung cancer.

The primary radiogenomic study is to build the correlation between gene mutations with semantic features on CT images. Rizzo et al.[110] found that the presence of pleural retraction, round tumor shape and pleural effusion are closely related to alterations in EGFR, KRAS and ALK, respectively. The development of computational features facilitates the quantitative prediction of gene mutations using machine learning methods[111]. For example, Song et al.[112] selected significant quantitative features and built a random forest model to predict ALK rearrangement. Tu et al.[113] extracted quantitative features to predict EGFR mutation with a logistic regression model, which achieved better performance compared with clinical and morphological features, and combining all these features together could achieve the best prediction results. PET/CT images are also involved in the prediction of gene mutation status[114, 115]. When multi-modality images are involved, these studies usually extract handcrafted features on each modality and concatenate them to make predictions.

Deep learning has also been applied to gene mutation predictions. Most studies focus on the mutation status of EGFR in NSCLC as the sample size is relatively large. Wang et al.[116] designed a DenseNet-based model to classify the EGFR mutation status of lung ADC and achieved better prediction performance than methods using predefined quantitative features. Wang et al.[116] visualized the saliency maps and observed that the CNN model paid attention to different tumor regions between the EGFR mutated and wildtype subtypes. Mu et al.[105] trained a CNN model similar to ResNet-18 to predict EGFR mutation in NSCLC and used the model output (named deep learning score) as a signature of the therapy response to EGFR tyrosine kinase inhibitors (EGFR-TKIs). There are also studies that built multi-task deep learning models to simultaneously predict EGFR mutation together with KRAS mutation[117] or programmed cell death ligand 1 (PD-L1) expression status[118, 119]. When using multi-modality images, each modality is used as a channel of the input of the CNN model, which keeps the topological structure of tumor images and facilitates the aggregation of local features. We summarized deep-learning radiomic studies on gene mutation prediction in Table 4.

Table 4 Summary of deep learning studies on gene mutation prediction

Study	Target gene	Image modality	Reported performance (AUC)
Dong et al.[117]	EGFR	CT	0.81
	KRAS		0.74
Wang et al.[116]	EGFR	CT	0.81
Wang et al.[118]	EGFR	CT	0.73
Wang et al.[119]	EGFR	CT	0.93
Zhao et al.[120]	EGFR	CT	0.75
Wang et al.[121]	EGFR	CT	0.88
Zhang et al.[122]	EGFR	CT	0.84
Gui et al.[123]	EGFR	CT	0.86
Mu et al.[105]	EGFR	FDG PET/CT	0.81
Yin et al.[124]	EGFR	FDG PET/CT	0.84

*The reported performances (AUC) may not be directly comparable among studies as the included patient cohorts are different.

Radiomics and functional gene sets

A functional gene set is a group of genes that share common biological functions[125]. Expression changes within some gene sets would cause abnormal cell functioning, which may further facilitate tumorigenesis. Scientists have found several cancer-related gene sets that control cell activities such as the cell cycle and glucose utilization[103]. It would be helpful if tumor-specific functional gene sets can be identified precisely to provide guidance for targeted therapies.

Scientists try to decode gene set alterations in lung cancer from medical images to find the relationship

between image features and biological pathways via functional gene sets. There are two categories of studies in this direction according to the division of gene sets. One category of studies adopts gene sets from pathway databases such as the kyoto encyclopedia of genes and genomes (KEGG)[126] and Molecular Signatures Database (MSigDB)[127]. For example, Grossmann et al.[128] ranked genes by the Spearman correlation of expression values with quantitative features and identified the correlated pathways for each quantitative feature using gene set enrichment analysis (GSEA)[125]. Grossmann et al.[128] observed that quantitative features such as texture entropy and voxel intensity variance features are associated with the immune system, the p53 pathway, and other pathways involved in cell cycle regulation. They also integrated radiomic, genomic and clinical information for better prognosis prediction[128]. Similar methods were also proposed to find pathways correlated with selected quantitative features[30] and/or the CT-derived signature[129]. Xia et al.[130] combined radiomic and deep features to build a "fused" signature that showed broader radiogenomic relationships with cancer-related pathways such as tumorigenesis. Different from studies using GSEA to obtain correlations, Smedley employed deep neural networks to predict quantitative features using gene sets, and the results showed that tumor texture features can be predicted from genes related to pathways such as AKT signaling and tumor necrosis factor[131].

Another category of studies groups genes by their expression patterns without involving prior knowledge of pathways. Genes are first grouped into highly co-expressed clusters according to their expressions, termed "metagenes" or "gene modules". Then, correlations between metagenes and quantitative features are examined. For example, Gaveart et al.[132] correlated semantic features extracted from CT images with the first principal component of each metagene and identified pathways in which each metagene is enriched. Gaveart et al.[132] also transferred such correlations to another dataset with patient's survival records to evaluate the prognostic value of semantic features using gene expression as a link. Zhou et al.[133] and Wang et al.[134] conducted experiments in a similar manner, focusing more on the biological meaning of image features instead of prognosis. Li et al.[135] used weight gene co-expression network analysis (WGCNA)[136] methods to identify metagenes, and then built a PET radiomic signature using the metagene that is closely associated with prognosis[135]. In these emerging studies that explore the connections between radiomics and biological pathways, the established connections can facilitate the interpretability and reliability of radiomics for prognosis prediction.

Radiogenomics links studies in computer science, radiology and biology, expands the clinical applications of radiomics and creates new possibilities for the future development of precision medicine. The development of radiogenomics is closely related to the progress of sequencing technologies, such as the next-generation sequencing (NGS)[137]. In recent years, single-cell genomics has played an increasingly important role in biological studies[138]. Single-cell gene expression unprecedently improves the resolution for cancer research and provides much more detailed information of tumors[139, 140]. The joint analysis of single-cell omics and radiomics is worth exploring in future studies.

4.4 Therapy response and prognostic prediction

Besides tumor phenotypes and genotypes, radiomics can also be applied to predict treatment effects and patient's prognoses. Early radiomic studies directly employed the survival time of patients as the clinical endpoint to evaluate the effectiveness of developed methods, including radiomic signatures, tumor habitat analysis and deep learning. For example, Aerts et al.[30] and Huang et al.[141] validated the prognostic value of the selected quantitative feature and the proposed radiomic signature, respectively. Wu et al.[48] identified a high-risk sub-region that is closely correlated with OS. Hosny et al.[142] built a deep learning model for lung cancer prognostication using CT images paired with OS data across multi-institute patient cohorts. As most patients diagnosed with lung cancer receive at least one type of therapy, recent studies have focused more on the prediction of the response and prognosis of certain therapy types, such as chemotherapy, radiotherapy, targeted therapy or immunotherapy. The non-invasive identification of patient groups that may benefit from a certain type of therapy will be of great help to the precision treatment of lung cancer.

Chemotherapy

Chemotherapy is a common treatment for lung cancer that uses certain drugs to kill cancer cells or stop them from spreading to other parts of the body. It is often used along with other therapies to improve its effectiveness. The treatment outcome is evaluated by the response status (whether there is tumor shrinkage or not), time to progression (TTP) and prognostic information such as OS, disease-free survival (DFS) and progression-free survival (PFS). The targets used for model training and validation can be either the same or different. For example, Coroller et al.[143] built a machine learning classifier using selected quantitative features to predict pathological complete response (pCR) and gross residual disease (GRD). Zhang et al.[144] constructed a radiomic signature to predict PFS. They validated the trained model on an additional patient cohort with the same clinical endpoint. Vaidya et al.[145] employed the histopathological image and genomic profiles to validate the obtained radiomic signature. Khorrami et al.[146] built a radiomic signature by predicting the pathological response

status and then associated the signature with OS and DFS. All the abovementioned studies focused on NSCLC, while Jain et al.[147] studied SCLC in a similar manner. We summarized typical radiomic studies on chemotherapy response for lung cancer treatment in Table 5.

Radiotherapy

Radiotherapy is another commonly used treatment strategy for lung cancer. It shrinks tumors by killing cancer cells with high-energy beams. Conventional and stereotactic are two major types of radiotherapy in terms of whether to apply beams from multiple angles. Radiotherapy is often used together with chemotherapy (also named as "chemoradiation"). Radiomic studies for radiotherapy are conducted in a similar manner as those for chemotherapy. Fried et al.[153] constructed a radiomic signature to predict OS after radiotherapy using features extracted from PET/CT images. Wu et al.[154] used the distant metastasis rate as the clinical endpoint and incorporated the histological subtype of tumors with a PET radiomic signature to build a more powerful model. Other non-radiomic information such as clinical information and counts of circulating tumor cells (CTCs)[155] were also used to improve the model performance. Scientists also employed longitudinal CT images in studies which provide more prognostic information. For example, Timmeren et al.[156] modeled the quantitative features along longitudinal CT scans with linear regression and then obtained the slope of each feature as new features to build the radiomic signature. There are also unsupervised methods used to assess therapy responses. Huynh et al.[157] performed unsupervised feature selection to identify quantitative features associated with OS, distant-metastasis-free survival (DMFS) and local-recurrence-free survival (LRFS). Li et al.[158] identified patient groups that potentially benefit from radiotherapy by a two-way clustering method. Table 6 summarizes typical radiomic studies on lung cancer radiotherapy responses.

It is worth noting that a new concept of "dosiomics" was introduced in radiotherapy analysis, which means using image features extracted from the planned treatment dose map to predict certain clinical endpoints. Dosiomic features can be used as prediction factors alone or integrated with quantitative features extracted from CT or PET images. Liang et al.[163] used texture features of the dose distribution map to predict the incidence of radiation pneumonitis (RP) after radiotherapy of lung cancer. Luo et al.[161] combined dosiomic statistics with quantitative features on core-beam CT (CBCT) images to predict tumor progression status and PFS. Dosiomics provides another modality of information based on human knowledge and experience, which is helpful to improve the prediction performance of radiomic models.

Current clinical practice of radiotherapy relies on manual or semi-manual planning for radiation dose. With the development of radiomics, automatic dose planning has become possible and attracts more and more attention during these years. The goal of studies on this topic is to deliver an adequate dose for the tumor while controlling the dose on other healthy organs at risk (OARs). Some studies try to plan the overall dose level to be de-

Table 5 Typical radiomic studies on chemotherapy response for lung cancer treatment

Study	Concurrent treatment	Image modality	Method	Primary target(s) for model development	Predicted clinical endpoint(s)	Including non-radiomic information
Coroller et al.[143]	Radiotherapy	CT	Radiomic classifier	Therapy response status	Therapy response status	Lymph node radiomics; Clinical information
Zhang et al.[144]	Radiotherapy	FDG PET/CT	Radiomic signature	PFS of patients	PFS of patients	No
Yang et al.[148]	EGFR targeted therapy	CECT	Radiomic signature	Therapy response status	Therapy response status	Clinical information
Chang et al.[149]	–	CT	Radiomic classifier	Therapy response status	Therapy response status	Clinical information
Khorrami et al.[146]	–	CT	Radiomic signature	Therapy response status	Therapy response status; OS and DFS of patients	Clinical and pathological information
Jong et al.[150]	–	CT	Raidomic signature	OS of patients	OS of patients	No
Jain et al.[147]	–	CT	Radiomic signature	OS of patients	OS and PFS of patients; Therapy response status	Clinical information
Vaidya et al.[145]	–	CT	Radiomic signature	DFS of patients	DFS of patients	Clinical information
Xie et al.[151]	–	CT	Radiomic signature	DFS of patients	DFS of patients	Clinical and pathological information
Khorrami et al.[152]	–	CT	Radiomic classifier and signature	Therapy response status	TTP and OS of patients	Clinical and pathological information

Table 6 Typical radiomic studies on radiotherapy response for lung cancer treatment

Study	Radiotherapy type	Image modality	Method	Primary target(s) for model development	Predicted clinical endpoint(s)	Including non-radiomic information
Wang et al.[159]	Conventional	CECT	Radiomic signature	OS of patients	OS of patients	Clinical information
Timmeren et al.[156]	Conventional	Longitudinal CBCT	Radiomic signature	OS and LRFS of patients	OS and LRFS of patients	No
Fried et al.[153]	Conventional	FDG PET/CT	Radiomic signature	OS of patients	OS of patients	Clinical information
Arshad et al.[160]	Conventional	FDG PET/CT	Radiomic signature	OS of patients	OS of patients	No
Huynh et al.[157]	Stereotactic	CT	Unsupervised quantitative feature selection	–	OS, DMFS and LRFS of patients	No
Jiao et al.[155]	Stereotactic	CT	Deep signature	RFS of patients	RFS of patients	Clinical information; CTC measurement
Luo et al.[161]	Stereotactic	CT	Radiomic classifier and signature	Tumor progression status	Tumor progression status and PFS of patients	Clinical and dosiomic information
Li et al.[162]	Stereotactic	CT (first follow-up)	Radiomic signature	OS, RFS and LRFS of patients	OS, RFS and LRFS of patients	Clinical information
Wu et al.[154]	Stereotactic	FDG PET/CT	Radiomic signature	Distant metastasis rate	Distant metastasis rate	Histological subtype
Li et al.[158]	Stereotactic	FDG PET/CT	Unsupervised clustering	–	OS and DFS of patients	No

livered. For example, Lou et al.[164] trained a deep learning model to predict the treatment outcome using pre-treatment CT volumes. They also added a decoder branch in the deep learning model to recover predefined quantitative features in order to supplement deep features. After that, they combined the model output with clinical variables to derive an individualized dose. Another type of study is to predict the dose level for each voxel. People usually adopt the U-Net structure and make some task-specific adjustments, such as using dense convolution[165] or adding cross-scale connections[166] to deal with this task. By setting the loss function to minimize the difference between the predicted dose and manually planned dose for each voxel, the deep learning model is trained to capture the dose-related features on the CT volume. These methods also employ the mask of planning target volume (PTV), OARs and beam setup information as guidance to make more accurate predictions on lesions and to avoid harming normal tissues.

Targeted therapy

Targeted therapy is a type of cancer treatment that targets certain gene mutations to directly inhibit cell proliferation, differentiation, migration, etc. During the past few years, the application of targeted therapy such as EGFR-TKI has greatly facilitated the development of precision medicine[167]. However, not all patients with the mutation would benefit from the treatment due to drug resistance. It would be helpful if the effectiveness of targeted therapy could be identified before the treatment. Radiomics provides a non-invasive tool to predict the therapy response, and most studies in lung cancer focus on EGFR-targeted therapies. Yang et al.[148] constructed a radiomic signature and incorporated the clinical information of patients to make predictions. Mu et al.[105] built a CNN model to predict EGFR mutation status, and then used the output of CNN as a deep signature to stratify patients according to their PFS. Song et al.[168] adopted the generative adversarial network (GAN) to extract deep features in a self-supervised manner. Song et al.[168] designed two generators, one of which is an encoder to obtain the deep feature vector from the original image and the other is a decoder to generate mimic images from a random noise vector. There are also two discriminators to distinguish both the image pairs and the vector pairs. They simultaneously trained the generators and discriminators, and then the deep features were used to build a signature for PFS with the LASSO model. Wang et al.[169] obtained deep features by predicting EGFR mutation status using a CNN model, and then these deep features were combined with clinical factors to build a prognostic signature by predicting PFS. Different from most studies that focus on the tumor area, they extracted features from the whole lung and suggested that the genotype and prognostic information could also be obtained from the area outside the tumor. Studies for ALK-related therapies are conducted using similar strategies with prognostic signatures or classifiers constructed using LASSO or CNN models[170–172]. Table 7 summarizes typical radiomic studies on the responses of lung cancer to targeted therapy.

Immunotherapy

Immunotherapy has emerged as an important new option for lung cancer treatment, especially for advanced or recalcitrant tumors[176, 177]. A majority of drugs for im-

Table 7 Typical radiomic studies on targeted therapy response for lung cancer treatment

Study	Targeted mutation	Image modality	Method	Primary target(s) for model development	Predicted clinical endpoint(s)	Including non-radiomic information
Tang et al.[173]	EGFR	CT	Radiomic predictor	PFS of patients	PFS of patients	Clinical information
Hou et al.[174]	EGFR	CT	Deep classifier	Tumor progression level	Tumor progression level	No
Song et al.[168]	EGFR	CT	Deep signature	PFS of patients	PFS of patients	No
Wang et al.[169]	EGFR	CT	Deep classifier and signature	EGFR mutation status and PFS of patients	PFS of patients	Clinical information
Yang et al.[148]	EGFR	CECT	Radiomic signature	Therapy response status	Therapy response status	Clinical information
Shao et al.[175]	EGFR	FDG PET/CT	Radiomic signature	PFS of patients	PFS of patients	Clinical information
Mu et al.[105]	EGFR	FDG PET/CT	Deep signature	EGFR mutation status	PFS of patients	No
Huang et al.[170]	ALK	CT	Radiomic signature	OS of patients	OS of patients	No
Song et al.[171]	ALK	CT	Deep classifier and signature	ALK fusion status	PFS of patients	Clinical and pathological information
Li et al.[172]	ALK	CECT	Radiomic signature	PFS of patients	PFS of patients	Clinical information

munotherapy are immune-checkpoint inhibitors that boost an antitumor immune response from T cells to find and attack the tumor[178]. Cytotoxic T lymphocyte antigen 4 (CTLA-4), programmed cell death protein 1 (PD-1) and PD-L1 are common targets for immunotherapy[179]. Clinical trials have shown the effectiveness of immunotherapy with significant improvement in patient survival[180]. Similar to other therapies, people also seek for non-invasive methods to identify patients who may potentially benefit from immunotherapy. Jazieh et al.[181] built a radiomic signature for immunotherapy by predicting PFS. Liu et al.[182] employed longitudinal CT images and calculated the absolute differences between features extracted on pretreatment and follow-up CT images, and then constructed a delta radiomic signature to predict therapy response status. Besides therapy response status and patient's prognosis, the genomic properties of tumors are also used as primary prediction targets for model development, such as tumor mutation burden[183], the expression status of PD-L1[184] and the mean expression of Granzyme A (GZMA) and perforin 1 (PRF1)[185]. These studies trained deep learning models and used the output of the trained model as the deep signature for prognostic analysis. Typical studies on immunotherapy response for lung cancer treatment are summarized in Table 8.

5 Software tools

There are some commonly-used open-source software tools in the field of radiomics that help researchers to carry out ideas and evaluate results. Some of them are desktop computer programs with easy operations and good interactivities. The others are packages developed to facilitate flexible implementation of algorithms using certain programming languages. In this section, we introduced two frequently-used desktop computer programs (ITK-SNAP[191] and 3D Slicer[192]) and took the most popular programming language Python[1] as an example to summarize typical packages used in lung cancer radiomic studies.

5.1 Desktop computer programs

In the radiomic analysis, desktop computer programs are efficient tools for medical image visualization and preprocessing. ITK-SNAP and 3D Slicer are two widely-used open-source desktop computer programs. Both of them provide multi-directional visualization of medical images from the axial, coronal and sagittal planes in the form of either 2D images or 3D reconstructed objects. Preprocessing steps such as denoising, gray-level windowing, resampling and image registration can be performed with a few clicks of the menu buttons. These computer programs also support semi-supervised tumor segmentation, in which users draw the approximate location of tumors as guidance, and then the plug-in algorithms automatically generate the tumor masks. The obtained tumor masks may not be ideal, and users can make modifications manually. The processed images and tumor masks can be saved for downstream analysis. The 3D Slicer also provides a Python scripting interface, which is convenient for users to write codes to implement the following feature extraction and clinical prediction steps using the same software.

5.2 Python packages

Python programming gives the choice of algorithms in each step of radiomic analysis to the users, making it possible to flexibly implement the programs according to the

[1] https://www.python.org

Table 8 Typical radiomic studies on immunotherapy response for lung cancer treatment

Study	Immunotherapy target(s)	Image modality	Method	Primary target(s) for model development	Predicted clinical endpoint(s)	Including non-radiomic information
Yang et al.[186]	PD-1	CT	Radiomic classifier and signature	Therapy response status	Therapy response status; PFS of patients	No
Trebeschi et al.[187]	PD-1	CECT	Radiomic signature	Therapy response status	Therapy response status; OS of patients	No
Wu et al.[188]	PD-1	CT & CECT	Radiomic signature	Therapy response status	Therapy response status	Clinical information
Liu et al.[182]	PD-1	Longitudinal CT	Delta radiomic signature	Therapy response status	Therapy response status	No
Jazieh et al.[181]	PD-L1	CT	Radiomic signature	PFS of patients	OS and PFS of patients	Clinical and pathological information
Tunali et al.[189]	PD-1/PD-L1	CECT	Radiomic classifier and signature	Therapy response status	Therapy response status; PFS of patients	Clinical information
Khorrami et al.[190]	PD-1/PD-L1	Longitudinal CT	Delta radiomic classifier and signature	Overall survival of patients	Therapy response status; OS of patients	No
Park et al.[185]	PD-1/PD-L1	FDG PET/CT	Deep signature	Mean expression of GZMA and PRF1	Therapy response status; OS and PFS of patients	No
He et al.[183]	Immune checkpoint(s)	CT	Deep signature	Tumor mutation burden (TMB) level	OS and PFS of patients	No
Mu et al.[184]	Immune checkpoint(s)	FDG PET/CT	Deep signature	Expression status of PD-L1	Therapy response status; OS and PFS of patients	No

data and tasks. In recent years, the Python community has wrapped many reusable code modules into packages with clear definitions of inputs and outputs. It becomes more and more convenient to conduct radiomic analysis using Python packages instead of writing codes from scratch. We summarized the commonly-used Python packages in lung cancer radiomics with the webpage of each package provided, as shown in Table 9.

The first step in image preprocessing is to load the medical images. People have developed pydicom[193], nibabel[194] and SimpleITK[195] to load the images stored in the dicom, NIFTI or both formats, respectively. After image loading, researchers can reduce the noises in images using the OpenCV[196] package, which is one of the most famous packages in computer vision. The gray-level windowing can be performed directly using the basic functions of Python. The resampling operation can be achieved with the SimpleITK or scipy[197] package to interpolate images to a certain size or voxel spacing. When multi-modality images are involved, researchers can align two images using the image registration packages SimpleElastix[198] or DEEDS[199].

In terms of tumor segmentation, the frequently-used nnU-Net[26] is a user-friendly package for both 2D and 3D segmentation tasks. This package is suitable for researchers with little experience in training deep learning models. There is no need to make the image sizes uniform prior to training, as nnU-Net itself would crop sub-volumes from the original image as inputs. Another convenience is that the hyper-parameters such as crop size, network architecture and training parameters are automatically configured. Users only need to transform images and labels to the NIFTI format and organize them according to the requirement of nnU-Net. Detailed instructions for using the package are available on the website (Table 9).

As for feature extraction, the most commonly used package is pyradiomics[32]. The calculation of predefined quantitative features is implemented in the package and feature values can be obtained with several lines of code. pyradiomics supports customized feature extraction by specifying the features to be included or excluded.

Among packages developed for clinical prediction, the scikit-learn[200] package is powerful in implementing non-deep-learning models. It also supports many machine learning operations such as feature selection, model training, evaluation metric calculation, and cross validation. Deep learning models are usually built by deep learning frameworks such as PyTorch[201] or TensorFlow. There are packages focusing on deep learning in medical images like MONAI[202] that developed on the top of existing frameworks. It becomes more quickly to implement classical models using MONAI as users only need to set a few model parameters without defining the model architecture layer by layer.

Besides the abovementioned tools, there are many other packages designed for similar purposes, developed

Table 9 Commonly-used Python packages in lung cancer radiomic studies

Category	Function	Package name	Webpage	Notes
Image preprocessing	Image input and output	Pydicom	https://pydicom.github.io	Designed for dicom files
		Nibabel	https://nipy.org/nibabel	Designed for NIFTI files
		SimpleITK	https://simpleitk.org	
	Image denoising	OpenCV	https://opencv.org	
	Image resampling	SimpleITK	https://simpleitk.org	
		Scipy	https://scipy.org/	
	Image registration	SimpleElastix	https://simpleelastix.github.io	Works together with SimpleITK
		DEEDS	https://github.com/mattiaspaul/deedsBCV	
Tumor segmentation	Segmentation mask generation	nnU-Net	https://github.com/MIC-DKFZ/nnUNet	Needs GPU(s) for training and prediction
Feature extraction	Predefined feature calculation	Pyradiomics	https://pyradiomics.readthedocs.io	Works together with SimpleITK
Clinical prediction	Training and evaluation of non-deep-learning models	Scikit-learn	https://scikit-learn.org	
	Training and evaluation of deep learning models	PyTorch	https://pytorch.org	
		Tensorflow	https://www.tensorflow.org	
	Fast implementation of deep learning procedures	MONAI	https://monai.io	Works together with PyTorch

on either Python or other programming languages such as MATLAB, R, etc. These packages and desktop computer programs greatly facilitate the scientific study of radiomics and make it possible to apply machine learning to cancer diagnosis in clinic.

6 Challenges and future directions

Radiomics is a rapidly developing field with many proposed methods and potential clinical applications. However, there are some challenges that may hinder the future advancement of radiomics research and applications, including the reproducibility of methods, insufficient labeled data and unclear causal relationships.

6.1 Improving study reproducibility

The most common challenge is the reproducibility of radiomic studies, especially across different institutions[203]. The predefined semantic and quantitative features introduced in Section 2.3 are frequently used in radiomic studies, but these features are sensitive to the steps in the radiomics workflow, such as image acquisition and tumor segmentation. Descriptive semantic features such as roundness and spiculation are highly dependent on the tumor segmentation and subjective judgments of the radiologist[31]. As for quantitative features, they are affected by the radiation dose and the choice of reconstruction algorithm[204]. Meyer et al.[205] checked the stability of 106 features and found that only 11.3% of them were reproduced for all tested radiation doses and CT reconstruction settings. Variations of quantitative features further decrease the reliability of radiomic signatures and the reproducibility of clinical predictions. Such issues are also encountered in deep learning studies[206]. There have been some efforts to compensate for the variations of quantitative feature values caused by different CT protocols[207]. Besides, the number and definition of quantitative features also vary a lot among different studies, making it hard to compare the performance between different methods. Different methods may even produce different feature values for the same image. To solve this issue, scientists have established the image biomarker standardization initiative (IBSI)[208] which aims to standardize the extraction of image features.

6.2 Handling insufficient labeled data

Another factor that restricts the performance of radiomic methods is the lack of labeled data[8]. Patient cohorts in radiomic studies are usually retrospectively collected, in which the paired images and clinical information are available for only a small group of patients[111]. Most radiomic methods are designed to work in a supervised manner. Insufficient training data would make such machine learning models fail to capture useful information from medical images or cause overfitting, especially in deep learning models[209]. Several strategies have been proposed to solve this issue. The simplest way is adding regularization terms in the loss function used to train the machine learning model, such as the LASSO and elastic-net methods. In deep learning, people also employ the dropout method in which some nodes (along with their

connections) are randomly dropped from the neural network during training to avoid overfitting[210]. A promising new strategy is model pretraining which employs self-supervised learning methods to better initialize model parameters, and then the model is fine-tuned with a small number of labeled data to achieve comparable performance with fully supervised training[27]. This type of model pretraining is suitable for the training of deep learning where a large dataset with few labeled data is available. Besides these two strategies, the federal learning framework may also be applied to incorporate training data from multiple institutes[211]. In federal learning, people do not need to collect data from different sources to build a single training set. Instead, the machine learning model with the same architecture can be distributed to multiple institutes to perform training on each institute. For each iteration during training, the gradients of parameters in each institute are transmitted to the central institute and the merged gradients are distributed to each institute again. In this way, the training set is enlarged with multi-source datasets. Federal learning can also be beneficial to solve the overfitting problem and protect data privacy[212].

6.3 Uncovering causal relationships

Currently, almost all radiomic studies make efforts to establish the correlation between image characteristics and clinical targets. But the correlation is usually built on given datasets and is often unstable when applied to other datasets. The reason is that two correlated factors may be simultaneously affected by other factors, which are called confounders. Different from correlation, the causality between factors characterizes the underlying biology of cancer and is not affected by confounders. Causality can be uncovered by causal inference methods[213], which may solve the issues of data scarcity and model robustness in radiomics. Castro et al.[214] discussed the importance of establishing the causal relationship between images and corresponding labels and offered step-by-step recommendations for future studies. More efforts should be made in the future, especially in establishing the correlation between tumor genotypes and clinical outcomes with the help of radiomics. Radiomics characterizes tumor phenotypes such as tumor size, shape and internal structures, which are affected by tumor genotypes and further affect treatment effect and patient's prognosis. With the development of imaging and sequencing technologies, scientists would obtain a deeper understanding of tumor properties from both macroscopic and microscopic levels. Radiomics serves as the link to uncover causal relationships between tumor phenotypes and genotypes, and helps to establish a comprehensive cross-scale mechanism of tumorigenesis and tumor progression in the future.

6.4 Summary

In this review, we summarized recent progress in radiomic studies. Radiomics has great potential in lung cancer diagnosis, although currently most radiomic studies are not applied to the real-world clinical decision-making. Besides improving the prediction performance, future AI-based radiomics should integrate more biological information of the tumor to provide interpretability for clinicians and patients. Clinical trials are also needed to validate these radiomic discoveries. On the basis of all these approaches, we believe that radiomics will step towards routine clinical practice and facilitate precision medicine in the future.

Acknowledgements

This work was supported by National Natural Science Foundation of China (No. 61721003) and the Tsinghua-Fuzhou Institute of Data Technologies, China (No. TFIDT 2021003).

Declarations of conflict of interest

The authors declared that they have no conflicts of interest to this work.

References

[1] R. S. Herbst, D. Morgensztern, C. Boshoff. The biology and management of non-small cell lung cancer. *Nature*, vol. 553, no. 7689, pp. 446–454, 2018. DOI: 10.1038/nature25183.

[2] H. Sung, J. Ferlay, R. L. Siegel, M. Laversanne, I. Soerjomataram, A. Jemal, F. Bray. Global cancer statistics 2020: GLOBOCAN estimates of incidence and mortality worldwide for 36 cancers in 185 countries. *CA: A Cancer Journal for Clinicians*, vol. 71, no. 3, pp. 209–249, 2021. DOI: 10.3322/caac.21660.

[3] M. Reck, K. F. Rabe. Precision diagnosis and treatment for advanced non-small-cell lung cancer. *The New England Journal of Medicine*, vol. 377, no. 9, pp. 849–861, 2017. DOI: 10.1056/NEJMra1703413.

[4] T. W. H. Meijer, L. F. de Geus-Oei, E. P. Visser, W. J. G. Oyen, M. G. Looijen-Salamon, D. Visvikis, A. F. T. M. Verhagen, J. Bussink, D. Vriens. Tumor delineation and quantitative assessment of glucose metabolic rate within histologic subtypes of non-small cell lung cancer by using dynamic.18F fluorodeoxyglucose PET. *Radiology*, vol. 283, no. 2, pp. 547–559, 2017. DOI: 10.1148/radiol.2016160329.

[5] G. Lee, S. H. Bak, H. Y. Lee. CT radiomics in thoracic oncology: Technique and clinical applications. *Nuclear Medicine and Molecular Imaging*, vol. 52, no. 2, pp. 91–98, 2018. DOI: 10.1007/s13139-017-0506-5.

[6] P. Lambin, E. Rios-Velazquez, R. Leijenaar, S. Carvalho, R. G. P. M. van Stiphout, P. Granton, C. M. L. Zegers, R. Gillies, R. Boellard, A. Dekker, H. J. W. L. Aerts. Radiomics: Extracting more information from medical images using advanced feature analysis. *European Journal of Cancer*, vol. 48, no. 4, pp. 441–446, 2012. DOI: 10.1016/j.ejca.2011.11.036.

[7] P. Lambin, R. T. H. Leijenaar, T. M. Deist, J. Peerlings, E. E. C. de Jong, J. van Timmeren, S. Sanduleanu, R. T. H. M. Larue, A. J. G. Even, A. Jochems, Y. van Wijk, H. Woodruff, J. Van Soest, T. Lustberg, E. Roelofs, W. van Elmpt, A. Dekker, F. M. Mottaghy, J. E. Wildberger, S. Walsh. Radiomics: The bridge between medical imaging and personalized medicine. *Nature Reviews Clinical Oncology*, vol. 14, no. 12, pp. 749–762, 2017. DOI: 10.1038/nrclinonc.2017.141.

[8] R. J. Gillies, P. E. Kinahan, H. Hricak. Radiomics: Images are more than pictures, they are data. *Radiology*, vol. 278, no. 2, pp. 563–577, 2016. DOI: 10.1148/radiol.2015151169.

[9] Y. LeCun, Y. Bengio, G. Hinton. Deep learning. *Nature*, vol. 521, no. 7553, pp. 436–444, 2015. DOI: 10.1038/nature14539.

[10] D. S. Kermany, M. Goldbaum, W. J. Cai, C. C. S. Valentim, H. Y. Liang, S. L. Baxter, A. Mckeown, G. Yang, X. K. Wu, F. B. Yan, J. Dong, M. K. Prasadha, J. Pei, M. Y. L. Ting, J. Zhu, C. Li, S. Hewett, J. Dong, I. Ziyar, A. Shi, R. Z. Zhang, L. H. Zheng, R. Hou, W. Shi, X. Fu, Y. O. Duan, V. A. N. Huu, C. Wen, E. D. Zhang, C. L. Zhang, O. L. Li, X. B. Wang, M. A. Singer, X. D. Sun, J. Xu, A. Tafreshi, M. A. Lewis, H. M. Xia, K. Zhang. Identifying medical diagnoses and treatable diseases by image-based deep learning. *Cell*, vol. 172, no. 5, pp. 1122–1131.e9, 1122. DOI: 10.1016/j.cell.2018.02.010.

[11] G. Litjens, T. Kooi, B. E. Bejnordi, A. A. A. Setio, F. Ciompi, M. Ghafoorian, J. A. W. M. Van Der laak, B. Van Ginneken, C. I. Sánchez. A survey on deep learning in medical image analysis. *Medical Image Analysis*, vol. 42, pp. 60–88, 2017. DOI: 10.1016/j.media.2017.07.005.

[12] M. Diwakar, M. Kumar. A review on CT image noise and its denoising. *Biomedical Signal Processing and Control*, vol. 42, pp. 73–88, 2018. DOI: 10.1016/j.bspc.2018.01.010.

[13] T. M. Lehmann, C. Gonner, K. Spitzer. Survey: Interpolation methods in medical image processing. *IEEE Transactions on Medical Imaging*, vol. 18, no. 11, pp. 1049–1075, 1999. DOI: 10.1109/42.816070.

[14] D. Mattes, D. R. Haynor, H. Vesselle, T. K. Lewellen, W. Eubank. PET-CT image registration in the chest using free-form deformations. *IEEE Transactions on Medical Imaging*, vol. 22, no. 1, pp. 120–128, 2003. DOI: 10.1109/TMI.2003.809072.

[15] H. J. Yu, X. R. Zhou, H. Y. Jiang, H. J. Kang, Z. G. Wang, T. Hara, H. Fujita. Learning 3D non-rigid deformation based on an unsupervised deep learning for PET/CT image registration. In *Proceedings of SPIE 10953, Medical Imaging 2019: Biomedical Applications in Molecular, Structural, and Functional Imaging*, San Diego, USA, pp. 439–444, 2019. DOI: 10.1117/12.2512698.

[16] E. Smistad, T. L. Falch, M. Bozorgi, A. C. Elster, F. Lindseth. Medical image segmentation on GPUs – A comprehensive review. *Medical Image Analysis*, vol. 20, no. 1, pp. 1–18, 2015. DOI: 10.1016/j.media.2014.10.012.

[17] M. Aljabri, M. AlGhamdi. A review on the use of deep learning for medical images segmentation. *Neurocomputing*, vol. 506, pp. 311–335, 2022. DOI: 10.1016/j.neucom.2022.07.070.

[18] M. Havaei, A. Davy, D. Warde-Farley, A. Biard, A. Courville, Y. Bengio, C. Pal, P. Jodoin, H. Larochelle. Brain tumor segmentation with Deep Neural Networks. *Medical Image Analysis*, vol. 35, pp. 18–31, 2017. DOI: 10.1016/j.media.2016.05.004.

[19] T. Messay, R. C. Hardie, S. K. Rogers. A new computationally efficient CAD system for pulmonary nodule detection in CT imagery. *Medical Image Analysis*, vol. 14, no. 3, pp. 390–406, 2010. DOI: 10.1016/j.media.2010.02.004.

[20] J. J. Suárez-Cuenca, W. Guo, Q. Li. Automated detection of pulmonary nodules in CT: False positive reduction by combining multiple classifiers. In *Proceedings of SPIE 7963, Medical Imaging 2011: Computer-Aided Diagnosis*, Lake Buena Vista (Orlando), USA, pp. 927–932, 2011. DOI: 10.1117/12.878793.

[21] M. Javaid, M. Javid, M. Z. U. Rehman, S. I. A. Shah. A novel approach to CAD system for the detection of lung nodules in CT images. *Computer Methods and Programs in Biomedicine*, vol. 135, pp. 125–139, 2016. DOI: 10.1016/j.cmpb.2016.07.031.

[22] J. Long, E. Shelhamer, T. Darrell. Fully convolutional networks for semantic segmentation. In *Proceedings of IEEE Conference on Computer Vision and Pattern Recognition*, Boston, USA, pp. 3431–3440, 2015. DOI: 10.1109/CVPR.2015.7298965.

[23] K. M. He, G. Gkioxari, P. Dollár, R. Girshick. Mask R-CNN. In *Proceedings of IEEE International Conference on Computer Vision*, Venice, Italy, pp. 2980–2988, 2017. DOI: 10.1109/ICCV.2017.322.

[24] O. Ronneberger, P. Fischer, T. Brox. U-Net: Convolutional networks for biomedical image segmentation. In *Proceedings of the 18th International Conference on Medical Image Computing and Computer-assisted Intervention*, Springer, Munich, Germany, pp. 234–241, 2015. DOI: 10.1007/978-3-319-24574-4_28.

[25] Ö. Ç içek, A. Abdulkadir, S. S. Lienkamp, T. Brox, O. Ronneberger. 3D U-Net: Learning dense volumetric segmentation from sparse annotation. In *Proceedings of the 19th International Conference on Medical Image Computing and Computer-Assisted Intervention*, Springer, Athens, Greece, pp. 424–432, 2016. DOI: 10.1007/978-3-319-46723-8_49.

[26] F. Isensee, P. F. Jaeger, S. A. A. Kohl, J. Petersen, K. H. Maier-Hein. nnU-Net: A self-configuring method for deep learning-based biomedical image segmentation. *Nature Methods*, vol. 18, no. 2, pp. 203–211, 2021. DOI: 10.1038/s41592-020-01008-z.

[27] X. Liu, F. J. Zhang, Z. Y. Hou, L. Mian, Z. Y. Wang, J. Zhang, J. Tang. Self-supervised learning: Generative or contrastive. *IEEE Transactions on Knowledge and Data Engineering*, vol. 35, no. 1, pp. 857–876. DOI: 10.1109/TKDE.2021.3090866.

[28] L. Chen, P. Bentley, K. Mori, K. Misawa, M. Fujiwara, D. Rueckert. Self-supervised learning for medical image analysis using image context restoration. *Medical Image Analysis*, vol. 58, Article number 101539, 2019. DOI: 10.1016/j.media.2019.101539.

[29] H. J. Lee, Y. T. Kim, C. H. Kang, B. S. Zhao, Y. Q. Tan, L. H. Schwartz, T. Persigehl, Y. K. Jeon, D. H. Chung. Epidermal growth factor receptor mutation in lung adenocarcinomas: Relationship with CT characteristics and histologic subtypes. *Radiology*, vol. 268, no. 1, pp. 254–264, 2013. DOI: 10.1148/radiol.13112553.

[30] H. J. W. L. Aerts, E. R. Velazquez, R. T. H. Leijenaar, C. Parmar, P. Grossmann, S. Carvalho, J. Bussink, R. Monshouwer, B. Haibe-Kains, D. Rietveld, F. Hoebers, M. M. Rietbergen, C. R. Leemans, A. Dekker, J. Quackenbush, R. J. Gillies, P. Lambin. Decoding tumour phenotype by noninvasive imaging using a quantitative radiomics ap-

proach. *Nature Communications*, vol. 5, Article number 4006, 2014. DOI: 10.1038/ncomms5006.

[31] M. R. Tomaszewski, R. J. Gillies. The biological meaning of radiomic features. *Radiology*, vol. 298, no. 3, pp. 505–516, 2021. DOI: 10.1148/radiol.2021202553.

[32] J. J. M. van Griethuysen, A. Fedorov, C. Parmar, A. Hosny, N. Aucoin, V. Narayan, R. G. H. Beets-Tan, J. C. Fillion-Robin, S. Pieper, H. J. W. L. Aerts. Computational radiomics system to decode the radiographic phenotype. *Cancer Research*, vol. 77, no. 21, pp. e104–e107, 2017. DOI: 10.1158/0008-5472.CAN-17-0339.

[33] A. Dosovitskiy, L. Beyer, A. Kolesnikov, D. Weissenborn, X. H. Zhai, T. Unterthiner, M. Dehghani, M. Minderer, G. Heigold, S. Gelly, J. Uszkoreit, N. Houlsby. An image is worth 16×16 words: Transformers for image recognition at scale, [Online], Available: https://openreview.net/forum?id=YicbFdNTTy, 2022.

[34] A. Vaswani, N. Shazeer, N. Parmar, J. Uszkoreit, L. Jones, A. N. Gomez, L. Kaiser, I. Polosukhin. Attention is all you need. In *Proceedings of the 31st Conference on Neural Information Processing Systems*, Long Beach, USA, pp. 6000–6010, 2017.

[35] S. Khan, M. Naseer, M. Hayat, S. W. Zamir, F. S. Khan, M. Shah. Transformers in vision: A survey. *ACM Computing Surveys*, vol. 54, no. 10s, Article number 200, 2022. DOI: 10.1145/3505244.

[36] F. Shamshad, S. Khan, S. W. Zamir, M. H. Khan, M. Hayat, F. S. Khan, H. Z. Fu. Transformers in medical imaging: A survey, [Online], Available: http://arxiv.org/abs/2201.09873, 2022.

[37] N. Papanikolaou, C. Matos, D. M. Koh. How to develop a meaningful radiomic signature for clinical use in oncologic patients. *Cancer Imaging*, vol. 20, no. 1, Article number 33, 2020. DOI: 10.1186/s40644-020-00311-4.

[38] R. Tibshirani. Regression shrinkage and selection via the lasso. *Journal of the Royal Statistical Society*: *Series B* (*Methodological*), vol. 58, no. 1, pp. 267–288, 1996. DOI: 10.1111/j.2517-6161.1996.tb02080.x.

[39] H. J. W. L. Aerts. The potential of radiomic-based phenotyping in precision medicine: A review. *JAMA Oncology*, vol. 2, no. 12, Article number 1636, 2016. DOI: 10.1001/jamaoncol.2016.2631.

[40] X. G. Zhang, X. Lu, Q. Shi, X. Q. Xu, H. C. E. Leung, L. N. Harris, J. D. Iglehart, A. Miron, J. S. Liu, W. H. Wong. Recursive SVM feature selection and sample classification for mass-spectrometry and microarray data. *BMC Bioinformatics*, vol. 7, Article number 197, 2006. DOI: 10.1186/1471-2105-7-197.

[41] I. Guyon, J. Weston, S. Barnhill, V. Vapnik. Gene selection for cancer classification using support vector machines. *Machine Learning*, vol. 46, no. 1, pp. 389–422, 2002. DOI: 10.1023/A:1012487302797.

[42] D. R. Cox. Regression models and life-tables. *Journal of the Royal Statistical Society*: *Series B* (*Methodological*), vol. 34, no. 2, pp. 187–202, 1972. DOI: 10.1111/j.2517-6161.1972.tb00899.x.

[43] K. Bera, N. Braman, A. Gupta, V. Velcheti, A. Madabhushi. Predicting cancer outcomes with radiomics and artificial intelligence in radiology. *Nature Reviews Clinical Oncology*, vol. 19, no. 2, pp. 132–146, 2022. DOI: 10.1038/s41571-021-00560-7.

[44] H. Kimura, R. D. Braun, E. T. Ong, R. Hsu, T. W. Secomb, D. Papahadjopoulos, K. Hong, M. W. Dewhirst. Fluctuations in red cell flux in tumor microvessels can lead to transient hypoxia and reoxygenation in tumor parenchyma. *Cancer Research*, vol. 56, no. 23, pp. 5522–5528, 1996.

[45] P. Carmeliet, R. K. Jain. Molecular mechanisms and clinical applications of angiogenesis. *Nature*, vol. 473, no. 7347, pp. 298–307, 2011. DOI: 10.1038/nature10144.

[46] M. R. Junttila, F. J. de Sauvage. Influence of tumour micro-environment heterogeneity on therapeutic response. *Nature*, vol. 501, no. 7467, pp. 346–354, 2013. DOI: 10.1038/nature12626.

[47] S. Napel, W. Mu, B. V. Jardim-Perassi, H. J. W. L. Aerts, R. J. Gillies. Quantitative imaging of cancer in the postgenomic era: Radio(geno)mics, deep learning, and habitats. *Cancer*, vol. 124, no. 24, pp. 4633–4649, 2018. DOI: 10.1002/cncr.31630.

[48] J. Wu, M. F. Gensheimer, X. Z. Dong, D. L. Rubin, S. Napel, M. Diehn, B. W. Loo, R. J. Li. Robust intratumor partitioning to identify high-risk subregions in lung cancer: A pilot study. *International Journal of Radiation Oncology Biology Physics*, vol. 95, no. 5, pp. 1504–1512, 2016. DOI: 10.1016/j.ijrobp.2016.03.018.

[49] A. J. G. Even, B. Reymen, M. D. La Fontaine, M. Das, F. M. Mottaghy, J. S. A. Belderbos, D. De Ruysscher, P. Lambin, W. van Elmpt. Clustering of multi-parametric functional imaging to identify high-risk subvolumes in non-small cell lung cancer. *Radiotherapy and Oncology*, vol. 125, no. 3, pp. 379–384, 2017. DOI: 10.1016/j.radonc.2017.09.041.

[50] R. Achanta, A. Shaji, K. Smith, A. Lucchi, P. Fua, S. Süsstrunk. SLIC superpixels compared to state-of-the-art superpixel methods. *IEEE Transactions on Pattern Analysis and Machine Intelligence*, vol. 34, no. 11, pp. 2274–2282, 2012. DOI: 10.1109/TPAMI.2012.120.

[51] L. Chen, K. F. Liu, X. Zhao, H. Shen, K. Zhao, W. T. Zhu. Habitat imaging-based.18F-FDG PET/CT radiomics for the preoperative discrimination of non-small cell lung cancer and benign inflammatory diseases. *Frontiers in Oncology*, vol. 11, Article number 759897, 2021. DOI: 10.3389/fonc.2021.759897.

[52] H. Shen, L. Chen, K. F. Liu, K. Zhao, J. S. Li, L. J. Yu, H. W. Ye, W. T. Zhu. A subregion-based positron emission tomography/computed tomography (PET/CT) radiomics model for the classification of non-small cell lung cancer histopathological subtypes. *Quantitative Imaging in Medicine and Surgery*, vol. 11, no. 7, pp. 2918–2932, 2021. DOI: 10.21037/qims-20-1182.

[53] D. Cherezov, D. Goldgof, L. Hall, R. Gillies, M. Schabath, H. Müller, A. Depeursinge. Revealing tumor habitats from texture heterogeneity analysis for classification of lung cancer malignancy and aggressiveness. *Scientific Reports*, vol. 9, no. 1, Article number 4500, 2019. DOI: 10.1038/s41598-019-38831-0.

[54] A. Marusyk, M. Janiszewska, K. Polyak. Intratumor heterogeneity: The Rosetta stone of therapy resistance. *Cancer Cell*, vol. 37, no. 4, pp. 471–484, 2020. DOI: 10.1016/j.ccell.2020.03.007.

[55] J. Q. Li, H. M. Lu, X. Fang, S. J. Chen, X. G. Zhang. Pixel-level clustering reveals intra-tumor heterogeneity in non-small cell lung cancer. In *Proceedings of IEEE International Conference on Bioinformatics and Biomedicine*, San Diego, USA, pp. 1536–1539, 2019. DOI: 10.1109/BIBM47256.2019.8983174.

[56] T. Caliński, J. Harabasz. A dendrite method for cluster

analysis. *Communications in Statistics*, vol. 3, no. 1, pp. 1–27, 1974. DOI: 10.1080/03610927408827101.

[57] R. Tibshirani, G. Walther, T. Hastie. Estimating the number of clusters in a data set via the gap statistic. *Journal of the Royal Statistical Society*: *Series B* (*Statistical Methodology*), vol. 63, no. 2, pp. 411–423, 2001. DOI: 10.1111/1467-9868.00293.

[58] A. Hosny, C. Parmar, J. Quackenbush, L. H. Schwartz, H. J. W. L. Aerts. Artificial intelligence in radiology. *Nature Reviews Cancer*, vol. 18, no. 8, pp. 500–510, 2018. DOI: 10.1038/s41568-018-0016-5.

[59] D. E. Rumelhart, G. E. Hinton, R. J. Williams. Learning representations by back-propagating errors. *Nature*, vol. 323, no. 6088, pp. 533–536, 1986. DOI: 10.1038/323533a0.

[60] P. Mobadersany, S. Yousefi, M. Amgad, D. A. Gutman, J. S. Barnholtz-Sloan, J. E. Velázquez Vega, D. J. Brat, L. A. D. Cooper. Predicting cancer outcomes from histology and genomics using convolutional networks. *Proceedings of the National Academy of Sciences of the United States of America*, vol. 115, no. 13, pp. E2970–E2979, 2018. DOI: 10.1073/pnas.1717139115.

[61] G. Chartrand, P. M. Cheng, E. Vorontsov, M. Drozdzal, S. Turcotte, C. J. Pal, S. Kadoury, A. Tang. Deep learning: A primer for radiologists. *RadioGraphics*, vol. 37, no. 7, pp. 2113–2131, 2017. DOI: 10.1148/rg.2017170077.

[62] J. Deng, W. Dong, R. Socher, L. J. Li, K. Li, L. Fei-Fei. ImageNet: A large-scale hierarchical image database. In *Proceedings of IEEE Conference on Computer Vision and Pattern Recognition*, Miami, USA, pp. 248–255, 2009. DOI: 10.1109/CVPR.2009.5206848.

[63] W. Shen, M. Zhou, F. Yang, D. Dong, C. Y. Yang, Y. L. Zang, J. Tian. Learning from experts: Developing transferable deep features for patient-level lung cancer prediction. In *Proceedings of the 19th International Conference on Medical Image Computing and Computer-assisted Intervention*, Springer, Athens, Greece, pp. 124–131, 2016. DOI: 10.1007/978-3-319-46723-8_15.

[64] Y. W. Xu, A. Hosny, R. Zeleznik, C. Parmar, T. Coroller, I. Franco, R. H. Mak, H. J. W. L. Aerts. Deep learning predicts lung cancer treatment response from serial medical imaging. *Clinical Cancer Research*, vol. 25, no. 11, pp. 3266–3275, 2019. DOI: 10.1158/1078-0432.CCR-18-2495.

[65] C. Larson. China's AI imperative. *Science*, vol. 359, no. 6376, pp. 628–630, 2018. DOI: 10.1126/science.359.6376.628.

[66] The National Lung Screening Trial Research Team. Reduced lung-cancer mortality with low-dose computed tomographic screening. *The New England Journal of Medicine*, vol. 365, no. 5, pp. 395–409, 2011. DOI: 10.1056/NEJMoa1102873.

[67] S. Hawkins, H. Wang, Y. Liu, A. Garcia, O. Stringfield, H. Krewer, Q. Li, D. Cherezov, R. A. Gatenby, Y. Balagurunathan, D. Goldgof, M. B. Schabath, L. Hall, R. J. Gillies. Predicting malignant nodules from screening CT scans. *Journal of Thoracic Oncology*, vol. 11, no. 12, pp. 2120–2128, 2016. DOI: 10.1016/j.jtho.2016.07.002.

[68] W. Wu, L. A. Pierce, Y. Z. Zhang, S. N. J. Pipavath, T. W. Randolph, K. J. Lastwika, P. D. Lampe, A. M. Houghton, H. N. Liu, L. M. Xia, P. E. Kinahan. Comparison of prediction models with radiological semantic features and radiomics in lung cancer diagnosis of the pulmonary nodules: A case-control study. *European Radiology*, vol. 29, no. 11, pp. 6100–6108, 2019. DOI: 10.1007/s00330-019-06213-9.

[69] Y. T. Xie, Y. Xia, J. P. Zhang, Y. Song, D. G. Feng, M. Fulham, W. D. Cai. Knowledge-based collaborative deep learning for benign-malignant lung nodule classification on chest CT. *IEEE Transactions on Medical Imaging*, vol. 38, no. 4, pp. 991–1004, 2019. DOI: 10.1109/TMI.2018.2876510.

[70] J. Wang, X. Liu, D. Dong, J. D. Song, M. Xu, Y. L. Zang, J. Tian. Prediction of malignant and benign of lung tumor using a quantitative radiomic method. In *Proceedings of the 38th Annual International Conference of the IEEE Engineering in Medicine and Biology Society*, Orlando, USA, pp. 1272–1275, 2016. DOI: 10.1109/EMBC.2016.7590938.

[71] N. Beig, M. Khorrami, M. Alilou, P. Prasanna, N. Braman, M. Orooji, S. Rakshit, K. Bera, P. Rajiah, J. Ginsberg, C. Donatelli, R. Thawani, M. Yang, F. Jacono, P. Tiwari, V. Velcheti, R. Gilkeson, P. Linden, A. Madabhushi. Perinodular and intranodular radiomic features on lung CT images distinguish adenocarcinomas from granulomas. *Radiology*, vol. 290, no. 3, pp. 783–792, 2019. DOI: 10.1148/radiol.2018180910.

[72] W. Shen, M. Zhou, F. Yang, D. D. Yu, D. Dong, C. Y. Yang, Y. L. Zang, J. Tian. Multi-crop convolutional neural networks for lung nodule malignancy suspiciousness classification. *Pattern Recognition*, vol. 61, pp. 663–673, 2017. DOI: 10.1016/j.patcog.2016.05.029.

[73] R. P. Zhang, L. Zhu, Z. T. Cai, W. Jiang, J. Li, C. W. Yang, C. X. Yu, B. Jiang, W. Wang, W. G. Xu, X. F. Chai, X. D. Zhang, Y. Tang. Potential feature exploration and model development based on.18F-FDG PET/CT images for differentiating benign and malignant lung lesions. *European Journal of Radiology*, vol. 121, Article number 108735, 2019. DOI: 10.1016/j.ejrad.2019.108735.

[74] S. Chen, S. Harmon, T. Perk, X. N. Li, M. J. Chen, Y. M. Li, R. Jeraj. Diagnostic classification of solitary pulmonary nodules using dual time.18F-FDG PET/CT image texture features in granuloma-endemic regions. *Scientific Reports*, vol. 7, no. 1, Article number 9370, 2017. DOI: 10.1038/s41598-017-08764-7.

[75] F. Kang, W. Mu, J. Gong, S. J. Wang, G. Q. Li, G. Y. Li, W. Qin, J. Tian, J. Wang. Integrating manual diagnosis into radiomics for reducing the false positive rate of.18F-FDG PET/CT diagnosis in patients with suspected lung cancer. *European Journal of Nuclear Medicine and Molecular Imaging*, vol. 46, no. 13, pp. 2770–2779, 2019. DOI: 10.1007/s00259-019-04418-0.

[76] Y. J. Park, D. Choi, J. Y. Choi, S. H. Hyun. Performance evaluation of a deep learning system for differential diagnosis of lung cancer with conventional CT and FDG PET/CT using transfer learning and metadata. *Clinical Nuclear Medicine*, vol. 46, no. 8, pp. 635–640, 2021. DOI: 10.1097/RLU.0000000000003661.

[77] R. S. Herbst, J. V. Heymach, S. M. Lippman. Lung cancer. *The New England Journal of Medicine*, vol. 359, no. 13, pp. 1367–1380, 2008. DOI: 10.1056/NEJMra0802714.

[78] Y. Qu, K. Emoto, T. Eguchi, R. G. Aly, H. Zheng, J. E. Chaft, K. S. Tan, D. R. Jones, M. G. Kris, P. S. Adusumilli, W. D. Travis. Pathologic assessment after neoadjuvant chemotherapy for NSCLC: Importance and implications of distinguishing adenocarcinoma from squamous cell carcinoma. *Journal of Thoracic Oncology*, vol. 14,

no. 3, pp. 482–493, 2019. DOI: 10.1016/j.jtho.2018.11.017.

[79] T. S. Mok, Y. L. Wu, S. Thongprasert, C. H. Yang, D. T. Chu, N. Saijo, P. Sunpaweravong, B. H. Han, B. Margono, Y. Ichinose, Y. Nishiwaki, Y. Ohe, J. J. Yang, B. Chewaskulyong, H. Y. Jiang, E. L. Duffield, C. L. Watkins, A. A. Armour, M. Fukuoka. Gefitinib or carboplatin-paclitaxel in pulmonary adenocarcinoma. *The New England Journal of Medicine*, vol. 361, no. 10, pp. 947–957, 2009. DOI: 10.1056/NEJMoa0810699.

[80] W. M. Wu, C. Parmar, P. Grossmann, J. Quackenbush, P. Lambin, J. Bussink, R. Mak, H. J. W. L. Aerts. Exploratory study to identify radiomics classifiers for lung cancer histology. *Frontiers in Oncology*, vol. 6, Article number 71, 2016. DOI: 10.3389/fonc.2016.00071.

[81] X. Z. Zhu, D. Dong, Z. D. Chen, M. J. Fang, L. W. Zhang, J. D. Song, D. D. Yu, Y. L. Zang, Z. Y. Liu, J. Y. Shi, J. Tian. Radiomic signature as a diagnostic factor for histologic subtype classification of non-small cell lung cancer. *European Radiology*, vol. 28, no. 7, pp. 2772–2778, 2018. DOI: 10.1007/s00330-017-5221-1.

[82] U. Bashir, B. Kawa, M. Siddique, S. M. Mak, A. Nair, E. Mclean, A. Bille, V. Goh, G. Cook. Non-invasive classification of non-small cell lung cancer: A comparison between random forest models utilising radiomic and semantic features. *The British Journal of Radiology*, vol. 92, no. 1099, Article number 20190159, 2019. DOI: 10.1259/bjr.20190159.

[83] X. Sha, G. Z. Gong, Q. T. Qiu, J. H. Duan, D. W. Li, Y. Yin. Identifying pathological subtypes of non-small-cell lung cancer by using the radiomic features of.18F-fluorodeoxyglucose positron emission computed tomography. *Translational Cancer Research*, vol. 8, no. 5, pp. 1741–1749, 2019. DOI: 10.21037/tcr.2019.08.20.

[84] S. H. Hyun, M. S. Ahn, Y. W. Koh, S. J. Lee. A machine-learning approach using PET-based radiomics to predict the histological subtypes of lung cancer. *Clinical Nuclear Medicine*, vol. 44, no. 12, pp. 956–960, 2019. DOI: 10.1097/RLU.0000000000002810.

[85] S. Koyasu, M. Nishio, H. Isoda, Y. Nakamoto, K. Togashi. Usefulness of gradient tree boosting for predicting histological subtype and EGFR mutation status of non-small cell lung cancer on.18F FDG-PET/CT. *Annals of Nuclear Medicine*, vol. 34, no. 1, pp. 49–57, 2020. DOI: 10.1007/s12149-019-01414-0.

[86] T. L. Chaunzwa, A. Hosny, Y. W. Xu, A. Shafer, N. Diao, M. Lanuti, D. C. Christiani, R. H. Mak, H. J. W. L. Aerts. Deep learning classification of lung cancer histology using CT images. *Scientific Reports*, vol. 11, no. 1, Article number 5471, 2021. DOI: 10.1038/s41598-021-84630-x.

[87] P. Marentakis, P. Karaiskos, V. Kouloulias, N. Kelekis, S. Argentos, N. Oikonomopoulos, C. Loukas. Lung cancer histology classification from CT images based on radiomics and deep learning models. *Medical & Biological Engineering & Computing*, vol. 59, no. 1, pp. 215–226, 2021. DOI: 10.1007/s11517-020-02302-w.

[88] Y. X. Guo, Q. Song, M. M. Jiang, Y. L. Guo, P. Xu, Y. Q. Zhang, C. C. Fu, Q. Fang, M. S. Zeng, X. Z. Yao. Histological subtypes classification of lung cancers on CT images using 3D deep learning and radiomics. *Academic Radiology*, vol. 28, no. 9, pp. e258–e266, 2021. DOI: 10.1016/j.acra.2020.06.010.

[89] L. Ubaldi, V. Valenti, R. F. Borgese, G. Collura, M. E. Fantacci, G. Ferrera, G. Iacoviello, B. F. Abbate, F. Laruina, A. Tripoli, A. Retico, M. Marrale. Strategies to develop radiomics and machine learning models for lung cancer stage and histology prediction using small data samples. *Physica Medica*, vol. 90, pp. 13–22, 2021. DOI: 10.1016/j.ejmp.2021.08.015.

[90] J. Liu, J. J. Cui, F. Liu, Y. X. Yuan, F. Guo, G. L. Zhang. Multi-subtype classification model for non-small cell lung cancer based on radiomics: SLS model. *Medical Physics*, vol. 46, no. 7, pp. 3091–3100, 2019. DOI: 10.1002/mp.13551.

[91] R. Patil, G. Mahadevaiah, A. Dekker. An approach toward automatic classification of tumor histopathology of non-small cell lung cancer based on radiomic features. *Tomography*, vol. 2, no. 4, pp. 374–377, 2016. DOI: 10.18383/j.tom.2016.00244.

[92] W. D. Travis, E. Brambilla, A. G. Nicholson, Y. Yatabe, J. H. M. Austin, M. B. Beasley, L. R. Chirieac, S. Dacic, E. Duhig, D. B. Flieder, K. Geisinger, F. R. Hirsch, Y. Ishikawa, K. M. Kerr, M. Noguchi, G. Pelosi, C. A. Powell, M. S. Tsao, I. Wistuba. The 2015 world health organization classification of lung tumors. *Journal of Thoracic Oncology*, vol. 10, no. 9, pp. 1243–1260, 2015. DOI: 10.1097/JTO.0000000000000630.

[93] C. Zhang, J. J. Zhang, F. P. Xu, Y. G. Wang, Z. Xie, J. Su, S. Dong, Q. Nie, Y. Shao, Q. Zhou, J. J. Yang, X. N. Yang, X. C. Zhang, Z. Li, Y. L. Wu, W. Z. Zhong. Genomic landscape and immune microenvironment features of preinvasive and early invasive lung adenocarcinoma. *Journal of Thoracic Oncology*, vol. 14, no. 11, pp. 1912–1923, 2019. DOI: 10.1016/j.jtho.2019.07.031.

[94] J. Gong, J. Y. Liu, W. Hao, S. D. Nie, S. P. Wang, W. J. Peng. Computer-aided diagnosis of ground-glass opacity pulmonary nodules using radiomic features analysis. *Physics in Medicine & Biology*, vol. 64, no. 13, Article number 135015, 2019. DOI: 10.1088/1361-6560/ab2757.

[95] X. Wang, Q. C. Li, J. L. Cai, W. Wang, P. Xu, Y. Q. Zhang, Q. Fang, C. C. Fu, L. Fan, Y. Xiao, S. Y. Liu. Predicting the invasiveness of lung adenocarcinomas appearing as ground-glass nodule on CT scan using multi-task learning and deep radiomics. *Translational Lung Cancer Research*, vol. 9, no. 4, pp. 1397–1406, 2020. DOI: 10.21037/tlcr-20-370.

[96] Y. L. She, L. Zhang, H. Y. Zhu, C. Y. Dai, D. Xie, H. K. Xie, W. Zhang, L. L. Zhao, L. L. Zou, K. Fei, X. W. Sun, C. Chen. The predictive value of CT-based radiomics in differentiating indolent from invasive lung adenocarcinoma in patients with pulmonary nodules. *European Radiology*, vol. 28, no. 12, pp. 5121–5128, 2018. DOI: 10.1007/s00330-018-5509-9.

[97] M. Yuan, Y. D. Zhang, X. H. Pu, Y. Zhong, H. Li, J. F. Wu, T. F. Yu. Comparison of a radiomic biomarker with volumetric analysis for decoding tumour phenotypes of lung adenocarcinoma with different disease-specific survival. *European Radiology*, vol. 27, no. 11, pp. 4857–4865, 2017. DOI: 10.1007/s00330-017-4855-3.

[98] H. H. Cho, G. Lee, H. Y. Lee, H. Park. Marginal radiomics features as imaging biomarkers for pathological invasion in lung adenocarcinoma. *European Radiology*, vol. 30, no. 5, pp. 2984–2994, 2020. DOI: 10.1007/s00330-019-06581-2.

[99] F. Y. Xu, W. C. Zhu, Y. Shen, J. Wang, R. Xu, C. Outesh, L. J. Song, Y. Gan, C. L. Pu, H. J. Hu. Radiomic-based quantitative CT analysis of pure ground-glass nodules to predict the invasiveness of lung adenocarcinoma. *Frontiers in Oncology*, vol. 10, Article number 872, 2020. DOI: 10.3389/fonc.2020.00872.

[100] L. Y. Wu, C. Gao, J. F. Ye, J. Y. Tao, N. Wang, P. P. Pang, P. Xiang, M. S. Xu. The value of various peritumoral radiomic features in differentiating the invasiveness of adenocarcinoma manifesting as ground-glass nodules. *European Radiology*, vol. 31, no. 12, pp. 9030–9037, 2021. DOI: 10.1007/s00330-021-07948-0.

[101] J. Cai, H. Liu, H. Yuan, Y. Wu, Q. Xu, Y. Lv, J. Li, J. Fu, J. Ye. A radiomics study to predict invasive pulmonary adenocarcinoma appearing as pure ground-glass nodules. *Clinical Radiology*, vol. 76, no. 2, pp. 143–151, 2021. DOI: 10.1016/j.crad.2020.10.005.

[102] W. F. Chen, M. Li, D. B. Mao, X. J. Ge, J. F. Wang, M. Y. Tan, W. L. Ma, X. M. Huang, J. J. Lu, C. Li, Y. Q. Hua, H. Wu. Radiomics signature on CECT as a predictive factor for invasiveness of lung adenocarcinoma manifesting as subcentimeter ground glass nodules. *Scientific Reports*, vol. 11, no. 1, Article number 3633, 2021. DOI: 10.1038/s41598-021-83167-3.

[103] V. L. Cox, P. Bhosale, G. R. Varadhachary, N. Wagner-Bartak, I. C. Glitza, K. A. Gold, J. T. Atkins, P. T. Soliman, D. S. Hong, A. Qayyum. Cancer genomics and important oncologic mutations: A contemporary guide for body imagers. *Radiology*, vol. 283, no. 2, pp. 314–340, 2017. DOI: 10.1148/radiol.2017152224.

[104] E. A. Ashley. Towards precision medicine. *Nature Reviews Genetics*, vol. 17, no. 9, pp. 507–522, 2016. DOI: 10.1038/nrg.2016.86.

[105] W. Mu, L. Jiang, J. Y. Zhang, Y. Shi, J. E. Gray, I. Tunali, C. Gao, Y. Y. Sun, J. Tian, X. M. Zhao, X. L. Sun, R. J. Gillies, M. B. Schabath. Non-invasive decision support for NSCLC treatment using PET/CT radiomics. *Nature Communications*, vol. 11, no. 1, Article number 5228, 2020. DOI: 10.1038/s41467-020-19116-x.

[106] A. Marusyk, V. Almendro, K. Polyak. Intra-tumour heterogeneity: A looking glass for cancer? *Nature Reviews Cancer*, vol. 12, no. 5, pp. 323–334, 2012. DOI: 10.1038/nrc3261.

[107] N. McGranahan, C. Swanton. Clonal heterogeneity and tumor evolution: Past, present, and the future. *Cell*, vol. 168, no. 4, pp. 613–628, 2017. DOI: 10.1016/j.cell.2017.01.018.

[108] L. M. Sholl, D. L. Aisner, M. Varella-Garcia, L. D. Berry, D. Dias-Santagata, I. I. Wistuba, H. D. Chen, J. Fujimoto, K. Kugler, W. A. Franklin, A. J. Iafrate, M. Ladanyi, M. G. Kris, B. E. Johnson, P. A. Bunn, J. D. Minna, D. J. Kwiatkowski. Multi-institutional oncogenic driver mutation analysis in lung adenocarcinoma: The lung cancer mutation consortium experience. *Journal of Thoracic Oncology*, vol. 10, no. 5, pp. 768–777, 2015. DOI: 10.1097/JTO.0000000000000516.

[109] Y. L. Wu, D. Planchard, S. Lu, H. Sun, N. Yamamoto, D. W. Kim, D. S. W. Tan, J. C. H. Yang, M. Azrif, T. Mitsudomi, K. Park, R. A. Soo, J. W. C. Chang, A. Alip, S. Peters, J. Y. Douillard. Pan-Asian adapted Clinical Practice Guidelines for the management of patients with metastatic non-small-cell lung cancer: A CSCO-ESMO initiative endorsed by JSMO, KSMO, MOS, SSO and TOS. *Annals of Oncology*, vol. 30, no. 2, pp. 171–210, 2019. DOI: 10.1093/annonc/mdy554.

[110] S. Rizzo, F. Petrella, V. Buscarino, F. De Maria, S. Raimondi, M. Barberis, C. Fumagalli, G. Spitaleri, C. Rampinelli, F. De Marinis, L. Spaggiari, M. Bellomi. CT radiogenomic characterization of EGFR, K-RAS, and ALK mutations in non-small cell lung cancer. *European Radiology*, vol. 26, no. 1, pp. 32–42, 2016. DOI: 10.1007/s00330-015-3814-0.

[111] Y. N. Qi, T. T. Zhao, M. Y. Han. The application of radiomics in predicting gene mutations in cancer. *European Radiology*, vol. 32, no. 6, pp. 4014–4024, 2022. DOI: 10.1007/s00330-021-08520-6.

[112] L. Song, Z. C. Zhu, L. Mao, X. L. Li, W. Han, H. Y. Du, H. W. Wu, W. Song, Z. Y. Jin. Clinical, conventional CT and radiomic feature-based machine learning models for predicting ALK rearrangement status in lung adenocarcinoma patients. *Frontiers in Oncology*, vol. 10, Article number 369, 2020. DOI: 10.3389/fonc.2020.00369.

[113] W. T. Tu, G. Y. Sun, L. Fan, Y. Wang, Y. Xia, Y. Guan, Q. Li, D. Zhang, S. Y. Liu, Z. B. Li. Radiomics signature: A potential and incremental predictor for EGFR mutation status in NSCLC patients, comparison with CT morphology. *Lung Cancer*, vol. 132, pp. 28–35, 2019. DOI: 10.1016/j.lungcan.2019.03.025.

[114] C. Chang, X. Y. Sun, G. Wang, H. Yu, W. L. Zhao, Y. Q. Ge, S. F. Duan, X. H. Qian, R. Wang, B. Lei, L. H. Wang, L. Liu, M. M. Ruan, H. Yan, C. Y. Liu, J. Chen, W. H. Xie. A machine learning model based on PET/CT radiomics and clinical characteristics predicts ALK rearrangement status in lung adenocarcinoma. *Frontiers in Oncology*, vol. 11, Article number 603882, 2021. DOI: 10.3389/fonc.2021.603882.

[115] J. Y. Zhang, X. M. Zhao, Y. Zhao, J. M. Zhang, Z. Q. Zhang, J. F. Wang, Y. C. Wang, M. Dai, J. Y. Han. Value of pre-therapy.18F-FDG PET/CT radiomics in predicting EGFR mutation status in patients with non-small cell lung cancer. *European Journal of Nuclear Medicine and Molecular Imaging*, vol. 47, no. 5, pp. 1137–1146, 2020. DOI: 10.1007/s00259-019-04592-1.

[116] S. Wang, J. Y. Shi, Z. X. Ye, D. Dong, D. D. Yu, M. Zhou, Y. Liu, O. Gevaert, K. Wang, Y. B. Zhu, H. Y. Zhou, Z. Y. Liu, J. Tian. Predicting EGFR mutation status in lung adenocarcinoma on computed tomography image using deep learning. *European Respiratory Journal*, vol. 53, no. 3, Article number 1800986, 2019. DOI: 10.1183/13993003.00986-2018.

[117] Y. Y. Dong, L. N. Hou, W. K. Yang, J. H. Han, J. W. Wang, Y. Qiang, J. J. Zhao, J. X. Hou, K. Song, Y. L. Ma, N. G. F. Kazihise, Y. F. Cui, X. T. Yang. Multi-channel multi-task deep learning for predicting *EGFR* and *KRAS* mutations of non-small cell lung cancer on CT images. *Quantitative Imaging in Medicine and Surgery*, vol. 11, no. 6, pp. 2354–2375, 2021. DOI: 10.21037/qims-20-600.

[118] C. D. Wang, X. Y. Xu, J. Shao, K. Zhou, K. F. Zhao, Y. Q. He, J. W. Li, J. X. Guo, Z. Yi, W. M. Li. Deep learning to predict EGFR mutation and PD-L1 expression status in non-small-cell lung cancer on computed tomography images. *Journal of Oncology*, vol. 2021, Article number 5499385, 2021. DOI: 10.1155/2021/5499385.

[119] C. D. Wang, J. C. Ma, J. Shao, S. Zhang, Z. N. Liu, Y. Z. Yu, W. M. Li. Predicting EGFR and PD-L1 status in NSCLC patients using multitask AI system based on CT images. *Frontiers in Immunology*, vol. 13, Article number 813072, 2022. DOI: 10.3389/fimmu.2022.813072.

[120] W. Zhao, J. C. Yang, B. B. Ni, D. X. Bi, Y. L. Sun, M. D. Xu, X. X. Zhu, C. Li, L. Jin, P. Gao, P. J. Wang, Y. Q. Hua, M. Li. Toward automatic prediction of *EGFR* mutation status in pulmonary adenocarcinoma with 3D deep learning. *Cancer Medicine*, vol. 8, no. 7, pp. 3532–3543, 2019. DOI: 10.1002/cam4.2233.

[121] L. S. Wang, S. Wang, H. Yu, Y. B. Zhu, W. M. Li, J.

Tian. A quarter-split domain-adaptive network for EGFR gene mutation prediction in lung cancer by standardizing heterogeneous CT image. In *Proceedings of the 43rd Annual International Conference of the IEEE Engineering in Medicine & Biology Society*, Mexico, pp. 3646–3649, 2021. DOI: 10.1109/EMBC46164.2021.9630395.

[122] B. H. Zhang, S. L. Qi, X. H. Pan, C. Li, Y. D. Yao, W. Qian, Y. B. Guan. Deep CNN model using CT radiomics feature mapping recognizes EGFR gene mutation status of lung adenocarcinoma. *Frontiers in Oncology*, vol. 10, Article number 598721, 2021. DOI: 10.3389/fonc.2020.598721.

[123] D. Q. Gui, Q. L. Song, B. Song, H. C. Li, M. H. Wang, X. H. Min, A. Li. AIR-Net: A novel multi-task learning method with auxiliary image reconstruction for predicting EGFR mutation status on CT images of NSCLC patients. *Computers in Biology and Medicine*, vol. 141, Article number 105157, 2022. DOI: 10.1016/j.compbiomed.2021.105157.

[124] G. T. Yin, Z. Y. Wang, Y. C. Song, X. F. Li, Y. W. Chen, L. Zhu, Q. Su, D. Dai, W. G. Xu. Prediction of EGFR mutation status based on.18F-FDG PET/CT imaging using deep learning-based model in lung adenocarcinoma. *Frontiers in Oncology*, vol. 11, Article number 709137, 2021. DOI: 10.3389/fonc.2021.709137.

[125] A. Subramanian, P. Tamayo, V. K. Mootha, S. Mukherjee, B. L. Ebert, M. A. Gillette, A. Paulovich, S. L. Pomeroy, T. R. Golub, E. S. Lander, J. P. Mesirov. Gene set enrichment analysis: A knowledge-based approach for interpreting genome-wide expression profiles. *Proceedings of the National Academy of Sciences of the United States of America*, vol. 102, no. 43, pp. 15545–15550, 2005. DOI: 10.1073/pnas.0506580102.

[126] M. Kanehisa, M. Furumichi, M. Tanabe, Y. Sato, K. Morishima. KEGG: New perspectives on genomes, pathways, diseases and drugs. *Nucleic Acids Research*, vol. 45, no. D1, pp. D353–D361, 2017. DOI: 10.1093/nar/gkw1092.

[127] A. Liberzon, C. Birger, H. Thorvaldsdóttir, M. Ghandi, J. P. Mesirov, P. Tamayo. The molecular signatures database hallmark gene set collection. *Cell Systems*, vol. 1, no. 6, pp. 417–425, 2015. DOI: 10.1016/j.cels.2015.12.004.

[128] P. Grossmann, O. Stringfield, N. El-Hachem, M. M. Bui, E. Rios Velazquez, C. Parmar, R. T. Leijenaar, B. Haibe-Kains, P. Lambin, R. J. Gillies, H. J. Aerts. Defining the biological basis of radiomic phenotypes in lung cancer. *eLife*, vol. 6, Article number e23421, 2017. DOI: 10.7554/eLife.23421.

[129] J. Lee, Y. Cui, X. L. Sun, B. L. Li, J. Wu, D. W. Li, M. F. Gensheimer, B. W. Loo, M. Diehn, R. J. Li. Prognostic value and molecular correlates of a CT image-based quantitative pleural contact index in early stage NSCLC. *European Radiology*, vol. 28, no. 2, pp. 736–746, 2018. DOI: 10.1007/s00330-017-4996-4.

[130] T. Xia, A. Kumar, M. Fulham, D. G. Feng, Y. Wang, E. Y. Kim, Y. Jung, J. Kim. Fused feature signatures to probe tumour radiogenomics relationships. *Scientific Reports*, vol. 12, no. 1, Article number 2173, 2022. DOI: 10.1038/s41598-022-06085-y.

[131] N. F. Smedley, D. R. Aberle, W. Hsu. Using deep neural networks and interpretability methods to identify gene expression patterns that predict radiomic features and histology in non-small cell lung cancer. *Journal of Medical Imaging*, vol. 8, no. 3, Article number 031906, 2021. DOI: 10.1117/1.JMI.8.3.031906.

[132] O. Gevaert, J. J. Xu, C. D. Hoang, A. N. Leung, Y. Xu, A. Quon, D. L. Rubin, S. Napel, S. K. Plevritis. Non-small cell lung cancer: Identifying prognostic imaging biomarkers by leveraging public gene expression microarray data-methods and preliminary results. *Radiology*, vol. 264, no. 2, pp. 387–396, 2012. DOI: 10.1148/radiol.12111607.

[133] M. Zhou, A. Leung, S. Echegaray, A. Gentles, J. B. Shrager, K. C. Jensen, G. J. Berry, S. K. Plevritis, D. L. Rubin, S. Napel, O. Gevaert. Non-small cell lung cancer radiogenomics map identifies relationships between molecular and imaging phenotypes with prognostic implications. *Radiology*, vol. 286, no. 1, pp. 307–315, 2018. DOI: 10.1148/radiol.2017161845.

[134] T. Wang, J. Gong, H. H. Duan, L. J. Wang, X. D. Ye, S. D. Nie. Correlation between CT based radiomics features and gene expression data in non-small cell lung cancer. *Journal of X-Ray Science and Technology*, vol. 27, no. 5, pp. 773–803, 2019. DOI: 10.3233/XST-190526.

[135] J. Li, Y. X. Liu, W. L. Dong, Y. Zhou, J. Q. Wu, K. Luan, L. S. Qi. Identifying.18F-FDG PET-metabolic radiomic signature for lung adenocarcinoma prognosis via the leveraging of prognostic transcriptomic module. *Quantitative Imaging in Medicine and Surgery*, vol. 12, no. 3, pp. 1893–1908, 2022. DOI: 10.21037/qims-21-706.

[136] P. Langfelder, S. Horvath. WGCNA: An R package for weighted correlation network analysis. *BMC Bioinformatics*, vol. 9, Article number 559, 2008. DOI: 10.1186/1471-2105-9-559.

[137] L. Shui, H. Y. Ren, X. Yang, J. Li, Z. W. Chen, C. Yi, H. Zhu, P. X. Shui. The era of radiogenomics in precision medicine: An emerging approach to support diagnosis, treatment decisions, and prognostication in oncology. *Frontiers in Oncology*, vol. 10, Article number 570465, 2021. DOI: 10.3389/fonc.2020.570465.

[138] N. Shah, J. Q. Li, F. H. Li, W. C. Chen, H. X. Gao, S. J. Chen, K. Hua, X. G. Zhang. An experiment on *ab initio* discovery of biological knowledge from scRNA-Seq data using machine learning. *Patterns*, vol. 1, no. 5, Article number 100071, 2020. DOI: 10.1016/j.patter.2020.100071.

[139] D. A. Lawson, K. Kessenbrock, R. T. Davis, N. Pervolarakis, Z. Werb. Tumour heterogeneity and metastasis at single-cell resolution. *Nature Cell Biology*, vol. 20, no. 12, pp. 1349–1360, 2018. DOI: 10.1038/s41556-018-0236-7.

[140] F. Y. Wu, J. Fan, Y. Y. He, A. W. Xiong, J. Yu, Y. X. Li, Y. Zhang, W. C. Zhao, F. Zhou, W. Li, J. Zhang, X. S. Zhang, M. Qiao, G. H. Gao, S. H. Chen, X. X. Chen, X. F. Li, L. K. Hou, C. Y. Wu, C. X. Su, S. X. Ren, M. Odenthal, R. Buettner, N. Fang, C. C. Zhou. Single-cell profiling of tumor heterogeneity and the microenvironment in advanced non-small cell lung cancer. *Nature Communications*, vol. 12, no. 1, Article number 2540, 2021. DOI: 10.1038/s41467-021-22801-0.

[141] Y. Q. Huang, Z. Y. Liu, L. He, X. Chen, D. Pan, Z. L. Ma, C. S. Liang, J. Tian, C. H. Liang. Radiomics signature: A potential biomarker for the prediction of disease-free survival in early-stage (I or II) non-small cell lung cancer. *Radiology*, vol. 281, no. 3, pp. 947–957, 2016. DOI: 10.1148/radiol.2016152234.

[142] A. Hosny, C. Parmar, T. P. Coroller, P. Grossmann, R. Zeleznik, A. Kumar, J. Bussink, R. J. Gillies, R. H. Mak, H. J. W. L. Aerts. Deep learning for lung cancer prognost-

ication: A retrospective multi-cohort radiomics study. *PLoS Medicine*, vol. 15, no. 11, Article number e1002711, 2018. DOI: 10.1371/journal.pmed.1002711.

[143] T. P. Coroller, V. Agrawal, E. Huynh, V. Narayan, S. W. Lee, R. H. Mak, H. J. W. L. Aerts. Radiomic-based pathological response prediction from primary tumors and lymph nodes in NSCLC. *Journal of Thoracic Oncology*, vol. 12, no. 3, pp. 467–476, 2017. DOI: 10.1016/j.jtho.2016.11.2226.

[144] N. S. Zhang, R. Liang, M. F. Gensheimer, M. Y. Guo, H. Zhu, J. M. Yu, M. Diehn, B. W. Loo, R. J. Li, J. Wu. Early response evaluation using primary tumor and nodal imaging features to predict progression-free survival of locally advanced non-small cell lung cancer. *Theranostics*, vol. 10, no. 25, pp. 11707–11718, 2020. DOI: 10.7150/thno.50565.

[145] P. Vaidya, K. Bera, A. Gupta, X. X. Wang, G. Corredor, P. F. Fu, N. Beig, P. Prasanna, P. D. Patil, P. D. Velu, P. Rajiah, R. Gilkeson, M. D. Feldman, H. Choi, V. Velcheti, A. Madabhushi. CT derived radiomic score for predicting the added benefit of adjuvant chemotherapy following surgery in stage I, II resectable non-small cell lung cancer: A retrospective multicohort study for outcome prediction. *The Lancet Digital Health*, vol. 2, no. 3, pp. e116–e128, 2020. DOI: 10.1016/S2589-7500(20)30002-9.

[146] M. Khorrami, P. Jain, K. Bera, M. Alilou, R. Thawani, P. Patil, U. Ahmad, S. Murthy, K. Stephans, P. F. Fu, V. Velcheti, A. Madabhushi. Predicting pathologic response to neoadjuvant chemoradiation in resectable stage III non-small cell lung cancer patients using computed tomography radiomic features. *Lung Cancer*, vol. 135, pp. 1–9, 2019. DOI: 10.1016/j.lungcan.2019.06.020.

[147] P. Jain, M. Khorrami, A. Gupta, P. Rajiah, K. Bera, V. S. Viswanathan, P. F. Fu, A. Dowlati, A. Madabhushi. Novel non-invasive radiomic signature on CT scans predicts response to platinum-based chemotherapy and is prognostic of overall survival in small cell lung cancer. *Frontiers in Oncology*, vol. 11, Article number 744724, 2021. DOI: 10.3389/fonc.2021.744724.

[148] F. C. Yang, J. Y. Zhang, L. Zhou, W. Xia, R. Zhang, H. F. Wei, J. X. Feng, X. Y. Zhao, J. M. Jian, X. Gao, S. H. Yuan. CT-based radiomics signatures can predict the tumor response of non-small cell lung cancer patients treated with first-line chemotherapy and targeted therapy. *European Radiology*, vol. 32, no. 3, pp. 1538–1547, 2022. DOI: 10.1007/s00330-021-08277-y.

[149] R. S. Chang, S. L. Qi, Y. Yue, X. Y. Zhang, J. D. Song, W. Qian. Predictive radiomic models for the chemotherapy response in non-small-cell lung cancer based on computerized-tomography images. *Frontiers in Oncology*, vol. 11, Article number 646190, 2021. DOI: 10.3389/fonc.2021.646190.

[150] E. E. C. de Jong, W. van Elmpt, S. Rizzo, A. Colarieti, G. Spitaleri, R. T. H. Leijenaar, A. Jochems, L. E. L. Hendriks, E. G. C. Troost, B. Reymen, A. M. C. Dingemans, P. Lambin. Applicability of a prognostic CT-based radiomic signature model trained on stage I-III non-small cell lung cancer in stage IV non-small cell lung cancer. *Lung Cancer*, vol. 124, pp. 6–11, 2018. DOI: 10.1016/j.lungcan.2018.07.023.

[151] D. Xie, T. T. Wang, S. J. Huang, J. J. Deng, Y. J. Ren, Y. Yang, J. Q. Wu, L. Zhang, K. Fei, X. W. Sun, Y. L. She, C. Chen. Radiomics nomogram for prediction disease-free survival and adjuvant chemotherapy benefits in patients with resected stage I lung adenocarcinoma. *Translational Lung Cancer Research*, vol. 9, no. 4, pp. 1112–1123, 2020. DOI: 10.21037/tlcr-19-577.

[152] M. Khorrami, M. Khunger, A. Zagouras, P. Patil, R. Thawani, K. Bera, P. Rajiah, P. F. Fu, V. Velcheti, A. Madabhushi. Combination of peri- and intratumoral radiomic features on baseline CT scans predicts response to chemotherapy in lung adenocarcinoma. *Radiology*: *Artificial Intelligence*, vol. 1, no. 2, Article number 180012, 2019. DOI: 10.1148/ryai.2019180012.

[153] D. V. Fried, O. Mawlawi, L. F. Zhang, X. Fave, S. H. Zhou, G. Ibbott, Z. X. Liao, L. E. Court. Stage III non-small cell lung cancer: Prognostic value of FDG PET quantitative imaging features combined with clinical prognostic factors. *Radiology*, vol. 278, no. 1, pp. 214–222, 2016. DOI: 10.1148/radiol.2015142920.

[154] J. Wu, T. Aguilera, D. Shultz, M. Gudur, D. L. Rubin, B. W. J. Loo, M. Diehn, R. J. Li. Early-stage non-small cell lung cancer: Quantitative imaging characteristics of.18F fluorodeoxyglucose PET/CT allow prediction of distant metastasis. *Radiology*, vol. 281, no. 1, pp. 270–278, 2016. DOI: 10.1148/radiol.2016151829.

[155] Z. C. Jiao, H. M. Li, Y. Xiao, J. Dorsey, C. B. Simone, S. Feigenberg, G. Kao, Y. Fan. Integration of deep learning radiomics and counts of circulating tumor cells improves prediction of outcomes of early stage NSCLC patients treated with stereotactic body radiation therapy. *International Journal of Radiation Oncology Biology Physics*, vol. 112, no. 4, pp. 1045–1054, 2022. DOI: 10.1016/j.ijrobp.2021.11.006.

[156] J. E. van Timmeren, W. van Elmpt, R. T. H. Leijenaar, B. Reymen, R. Monshouwer, J. Bussink, L. Paelinck, E. Bogaert, C. De Wagter, E. Elhaseen, Y. Lievens, O. Hansen, C. Brink, P. Lambin. Longitudinal radiomics of cone-beam CT images from non-small cell lung cancer patients: Evaluation of the added prognostic value for overall survival and locoregional recurrence. *Radiotherapy and Oncology*, vol. 136, pp. 78–85, 2019. DOI: 10.1016/j.radonc.2019.03.032.

[157] E. Huynh, T. P. Coroller, V. Narayan, V. Agrawal, Y. Hou, J. Romano, I. Franco, R. H. Mak, H. J. W. L. Aerts. CT-based radiomic analysis of stereotactic body radiation therapy patients with lung cancer. *Radiotherapy and Oncology*, vol. 120, no. 2, pp. 258–266, 2016. DOI: 10.1016/j.radonc.2016.05.024.

[158] H. M. Li, M. Galperin-Aizenberg, D. Pryma, C. B. Simone, Y. Fan. Unsupervised machine learning of radiomic features for predicting treatment response and overall survival of early stage non-small cell lung cancer patients treated with stereotactic body radiation therapy. *Radiotherapy and Oncology*, vol. 129, no. 2, pp. 218–226, 2018. DOI: 10.1016/j.radonc.2018.06.025.

[159] L. L. Wang, T. T. Dong, B. W. Xin, C. R. Xu, M. Y. Guo, H. Q. Zhang, D. G. Feng, X. Y. Wang, J. M. Yu. Integrative nomogram of CT imaging, clinical, and hematological features for survival prediction of patients with locally advanced non-small cell lung cancer. *European Radiology*, vol. 29, no. 6, pp. 2958–2967, 2019. DOI: 10.1007/s00330-018-5949-2.

[160] M. A. Arshad, A. Thornton, H. N. Lu, H. Tam, K. Wallitt, N. Rodgers, A. Scarsbrook, G. Mcdermott, G. J. Cook, D. Landau, S. Chua, R. O'connor, J. Dickson, D. A. Power, T. D. Barwick, A. Rockall, E. O. Aboagye. Discovery of pre-therapy 2-deoxy-2-^{18}F-fluoro-D-glucose positron emission tomography-based radiomics classifiers of survival outcome in non-small-cell lung cancer patients. *European Journal of Nuclear Medicine and Mo-*

lecular Imaging, vol. 46, no. 2, pp. 455–466, 2019. DOI: 10.1007/s00259-018-4139-4.

[161] L. M. Luo, B. T. Huang, C. Z. Chen, Y. Wang, C. H. Su, G. B. Peng, C. B. Zeng, Y. X. Wu, R. H. Wang, K. Huang, Z. H. Qiu. A combined model to improve the prediction of local control for lung cancer patients undergoing stereotactic body radiotherapy based on radiomic signature plus clinical and dosimetric parameters. *Frontiers in Oncology*, vol. 11, Article number 819047, 2022. DOI: 10.3389/fonc.2021.819047.

[162] Q. Li, J. Kim, Y. Balagurunathan, J. Qi, Y. Liu, K. Latifi, E. G. Moros, M. B. Schabath, Z. X. Ye, R. J. Gillies, T. J. Dilling. CT imaging features associated with recurrence in non-small cell lung cancer patients after stereotactic body radiotherapy. *Radiation Oncology*, vol. 12, no. 1, Article number 158, 2017. DOI: 10.1186/s13014-017-0892-y.

[163] B. Liang, H. Yan, Y. Tian, X. Y. Chen, L. L. Yan, T. Zhang, Z. M. Zhou, L. Wang, J. R. Dai. Dosiomics: Extracting 3D spatial features from dose distribution to predict incidence of radiation pneumonitis. *Frontiers in Oncology*, vol. 9, Article number 269, 2019. DOI: 10.3389/fonc.2019.00269.

[164] B. Lou, S. Doken, T. L. Zhuang, D. Wingerter, M. Gidwani, N. Mistry, L. Ladic, A. Kamen, M. E. Abazeed. An image-based deep learning framework for individualising radiotherapy dose: A retrospective analysis of outcome prediction. *The Lancet Digital Health*, vol. 1, no. 3, pp. e136–e147, 2019. DOI: 10.1016/S2589-7500(19)30058-5.

[165] A. M. Barragán-Montero, D. Nguyen, W. G. Lu, M. H. Lin, R. Norouzi-Kandalan, X. Geets, E. Sterpin, S. Jiang. Three-dimensional dose prediction for lung IMRT patients with deep neural networks: Robust learning from heterogeneous beam configurations. *Medical Physics*, vol. 46, no. 8, pp. 3679–3691, 2019. DOI: 10.1002/mp.13597.

[166] Y. Li, K. H. He, M. W. Ma, X. Qi, Y. Bai, S. W. Liu, Y. Gao, F. Lyu, C. H. Jia, B. Zhao, X. S. Gao. Using deep learning to model the biological dose prediction on bulky lung cancer patients of partial stereotactic ablation radiotherapy. *Medical Physics*, vol. 47, no. 12, pp. 6540–6550, 2020. DOI: 10.1002/mp.14518.

[167] M. Maemondo, A. Inoue, K. Kobayashi, S. Sugawara, S. Oizumi, H. Isobe, A. Gemma, M. Harada, H. Yoshizawa, I. Kinoshita, Y. Fujita, S. Okinaga, H. Hirano, K. Yoshimori, T. Harada, T. Ogura, M. Ando, H. Miyazawa, T. Tanaka, Y. Saijo, K. Hagiwara, S. Morita, T. Nukiwa, North-East Japan Study Group. Gefitinib or chemotherapy for non-small-cell lung cancer with mutated EGFR. *The New England Journal of Medicine*, vol. 362, no. 25, pp. 2380–2388, 2010. DOI: 10.1056/NEJMoa0909530.

[168] J. D. Song, L. Wang, N. N. Ng, M. F. Zhao, J. Y. Shi, N. Wu, W. M. Li, Z. Y. Liu, K. W. Yeom, J. Tian. Development and validation of a machine learning model to explore tyrosine kinase inhibitor response in patients with stage IV *EGFR* variant-positive non-small cell lung cancer. *JAMA Network Open*, vol. 3, no. 12, Article number e2030442, 2020. DOI: 10.1001/jamanetworkopen.2020.30442.

[169] S. Wang, H. Yu, Y. C. Gan, Z. J. Wu, E. C. Li, X. H. Li, J. X. Cao, Y. B. Zhu, L. S. Wang, H. Deng, M. Xie, Y. Y. Wang, X. D. Ma, D. Liu, B. J. Chen, P. W. Tian, Z. X. Qiu, J. H. Xian, J. Ren, K. Wang, W. Wei, F. Xie, Z. H. Li, Q. Wang, X. Y. Xue, Z. Y. Liu, J. Y. Shi, W. M. Li, J. Tian. Mining whole-lung information by artificial intelligence for predicting EGFR genotype and targeted therapy response in lung cancer: A multicohort study. *The Lancet Digital Health*, vol. 4, no. 5, pp. e309–e319, 2022. DOI: 10.1016/S2589-7500(22)00024-3.

[170] L. Huang, J. Y. Chen, W. G. Hu, X. Y. Xu, D. Liu, J. M. Wen, J. Y. Lu, J. Z. Cao, J. H. Zhang, Y. Gu, J. Z. Wang, M. Fan. Assessment of a radiomic signature developed in a general NSCLC cohort for predicting overall survival of ALK-positive patients with different treatment types. *Clinical Lung Cancer*, vol. 20, no. 6, pp. e638–e651, 2019. DOI: 10.1016/j.cllc.2019.05.005.

[171] Z. B. Song, T. C. Liu, L. Shi, Z. Y. Yu, Q. Shen, M. D. Xu, Z. Z. Huang, Z. J. Cai, W. X. Wang, C. W. Xu, J. J. Sun, M. Chen. The deep learning model combining CT image and clinicopathological information for predicting ALK fusion status and response to ALK-TKI therapy in non-small cell lung cancer patients. *European Journal of Nuclear Medicine and Molecular Imaging*, vol. 48, no. 2, pp. 361–371, 2021. DOI: 10.1007/s00259-020-04986-6.

[172] H. L. Li, R. Zhang, S. W. Wang, M. J. Fang, Y. B. Zhu, Z. H. Hu, D. Dong, J. Y. Shi, J. Tian. CT-based radiomic signature as a prognostic factor in stage IV *ALK*-positive non-small-cell lung cancer treated with TKI crizotinib: A proof-of-concept study. *Frontiers in Oncology*, vol. 10, Article number 57, 2020. DOI: 10.3389/fonc.2020.00057.

[173] X. Tang, Y. Li, W. F. Yan, W. L. Qian, T. Pang, Y. L. Gong, Z. G. Yang. Machine learning-based CT radiomics analysis for prognostic prediction in metastatic non-small cell lung cancer patients with *EGFR*-T790M mutation receiving third-generation EGFR-TKI osimertinib treatment. *Frontiers in Oncology*, vol. 11, Article number 719919, 2021. DOI: 10.3389/fonc.2021.719919.

[174] R. P. Hou, X. Y. Li, J. F. Xiong, T. L. Shen, W. Yu, L. H. Schwartz, B. S. Zhao, J. Zhao, X. L. Fu. Predicting tyrosine kinase inhibitor treatment response in stage IV lung adenocarcinoma patients with EGFR mutation using model-based deep transfer learning. *Frontiers in Oncology*, vol. 11, Article number 679764, 2021. DOI: 10.3389/fonc.2021.679764.

[175] D. Shao, D. Y. Du, H. P. Liu, J. Q. Lv, Y. Cheng, H. Zhang, W. B. Lv, S. X. Wang, L. J. Lu. Identification of stage IIIC/IV EGFR-mutated non-small cell lung cancer populations sensitive to targeted therapy based on a PET/CT radiomics risk model. *Frontiers in Oncology*, vol. 11, Article number 721318, 2021. DOI: 10.3389/fonc.2021.721318.

[176] S. Kruger, M. Ilmer, S. Kobold, B. L. Cadilha, S. Endres, S. Ormanns, G. Schuebbe, B. W. Renz, J. G. D'haese, H. Schloesser, V. Heinemann, M. Subklewe, S. Boeck, J. Werner, M. von Bergwelt-baildon. Advances in cancer immunotherapy 2019 – latest trends. *Journal of Experimental & Clinical Cancer Research*, vol. 38, no. 1, Article number 268, 2019. DOI: 10.1186/s13046-019-1266-0.

[177] D. W. S. Mak, S. Li, A. Minchom. Challenging the recalcitrant disease-developing molecularly driven treatments for small cell lung cancer. *European Journal of Cancer*, vol. 119, pp. 132–150, 2019. DOI: 10.1016/j.ejca.2019.04.037.

[178] F. F. Teng, X. J. Meng, L. Kong, J. M. Yu. Progress and challenges of predictive biomarkers of anti PD-1/PD-L1 immunotherapy: A systematic review. *Cancer Letters*, vol. 414, pp. 166–173, 2018. DOI: 10.1016/j.canlet.2017.11.014.

[179] C. Zhang, L. de A. F. Fonseca, Z. W. Shi, C. Zhu, A. Dekker, I. Bermejo, L. Wee. Systematic review of radiomic

biomarkers for predicting immune checkpoint inhibitor treatment outcomes. *Methods*, vol. 188, pp. 61–72, 2021. DOI: 10.1016/j.ymeth.2020.11.005.

[180] L. Fehrenbacher, A. Spira, M. Ballinger, M. Kowanetz, J. Vansteenkiste, J. Mazieres, K. Park, D. Smith, A. Artal-Cortes, C. Lewanski, F. Braiteh, D. Waterkamp, P. He, W. Zou, D. S. Chen, J. Yi, A. Sandler, A. Rittmeyer. Atezolizumab versus docetaxel for patients with previously treated non-small-cell lung cancer (POPLAR): A multicentre, open-label, phase 2 randomised controlled trial. *The Lancet*, vol. 387, no. 10030, pp. 1837–1846, 2016. DOI: 10.1016/S0140-6736(16)00587-0.

[181] K. Jazieh, M. Khorrami, A. Saad, M. Gad, A. Gupta, P. Patil, V. S. Viswanathan, P. Rajiah, C. J. Nock, M. Gilkey, P. F. Fu, N. A. Pennell, A. Madabhushi. Novel imaging biomarkers predict outcomes in stage III unresectable non-small cell lung cancer treated with chemoradiation and durvalumab. *Journal for ImmunoTherapy of Cancer*, vol. 10, no. 3, Article number e003778, 2022. DOI: 10.1136/jitc-2021-003778.

[182] Y. Liu, M. H. Wu, Y. W. Zhang, Y. H. Luo, S. He, Y. N. Wang, F. Chen, Y. L. Liu, Q. Yang, Y. Y. Li, H. Wei, H. Zhang, C. W. Jin, N. Lu, W. H. Li, S. C. Wang, Y. Guo, Z. X. Ye. Imaging biomarkers to predict and evaluate the effectiveness of immunotherapy in advanced non-small-cell lung cancer. *Frontiers in Oncology*, vol. 11, Article number 657615, 2021. DOI: 10.3389/fonc.2021.657615.

[183] B. X. He, D. Dong, Y. L. She, C. C. Zhou, M. J. Fang, Y. B. Zhu, H. H. Zhang, Z. P. Huang, T. Jiang, J. Tian, C. Chen. Predicting response to immunotherapy in advanced non-small-cell lung cancer using tumor mutational burden radiomic biomarker. *Journal for ImmunoTherapy of Cancer*, vol. 8, no. 2, Article number e000550, 2020. DOI: 10.1136/jitc-2020-000550.

[184] W. Mu, L. Jiang, Y. Shi, I. Tunali, J. E. Gray, E. Katsoulakis, J. Tian, R. J. Gillies, M. B. Schabath. Non-invasive measurement of PD-L1 status and prediction of immunotherapy response using deep learning of PET/CT images. *Journal for ImmunoTherapy of Cancer*, vol. 9, no. 6, Article number e002118, 2021. DOI: 10.1136/jitc-2020-002118.

[185] C. Park, K. J. Na, H. Choi, C. Y. Ock, S. Ha, M. Kim, S. Park, B. Keam, T. M. Kim, J. C. Paeng, I. K. Park, C. H. Kang, D. W. Kim, G. J. Cheon, K. W. Kang, Y. T. Kim, D. S. Heo. Tumor immune profiles noninvasively estimated by FDG PET with deep learning correlate with immunotherapy response in lung adenocarcinoma. *Theranostics*, vol. 10, no. 23, pp. 10838–10848, 2020. DOI: 10.7150/thno.50283.

[186] B. Yang, L. Zhou, J. Zhong, T. F. Lv, A. Li, L. Ma, J. Zhong, S. S. Yin, L. T. Huang, C. S. Zhou, X. Y. Li, Y. Q. Ge, X. W. Tao, L. J. Zhang, Y. Son, G. M. Lu. Combination of computed tomography imaging-based radiomics and clinicopathological characteristics for predicting the clinical benefits of immune checkpoint inhibitors in lung cancer. *Respiratory Research*, vol. 22, no. 1, Article number 189, 2021. DOI: 10.1186/s12931-021-01780-2.

[187] S. Trebeschi, S. G. Drago, N. J. Birkbak, I. Kurilova, A. M. Călin, A. Delli Pizzi, F. Lalezari, D. M. J. Lambregts, M. W. Rohaan, C. Parmar, E. A. Rozeman, K. J. Hartemink, C. Swanton, J. B. A. G. Haanen, C. U. Blank, E. F. Smit, R. G. H. Beets-Tan, H. J. W. L. Aerts. Predicting response to cancer immunotherapy using noninvasive radiomic biomarkers. *Annals of Oncology*, vol. 30, no. 6, pp. 998–1004, 2019. DOI: 10.1093/annonc/mdz108.

[188] M. H. Wu, Y. Y. Zhang, J. N. Zhang, Y. W. Zhang, Y. N. Wang, F. Chen, Y. H. Luo, S. He, Y. L. Liu, Q. Yang, Y. Y. Li, H. Wei, H. Zhang, N. Lu, S. C. Wang, Y. Guo, Z. X. Ye, Y. Liu. A combined-radiomics approach of CT images to predict response to anti-PD-1 immunotherapy in NSCLC: A retrospective multicenter study. *Frontiers in Oncology*, vol. 11, Article number 688679, 2022. DOI: 10.3389/fonc.2021.688679.

[189] I. Tunali, J. E. Gray, J. Qi, M. Abdalah, D. K. Jeong, A. Guvenis, R. J. Gillies, M. B. Schabath. Novel clinical and radiomic predictors of rapid disease progression phenotypes among lung cancer patients treated with immunotherapy: An early report. *Lung Cancer*, vol. 129, pp. 75–79, 2019. DOI: 10.1016/j.lungcan.2019.01.010.

[190] M. Khorrami, P. Prasanna, A. Gupta, P. Patil, P. D. Velu, R. Thawani, G. Corredor, M. Alilou, K. Bera, P. F. Fu, M. Feldman, V. Velcheti, A. Madabhushi. Changes in CT radiomic features associated with lymphocyte distribution predict overall survival and response to immunotherapy in non-small cell lung cancer. *Cancer Immunology Research*, vol. 8, no. 1, pp. 108–119, 2020. DOI: 10.1158/2326-6066.CIR-19-0476.

[191] P. A. Yushkevich, J. Piven, H. C. Hazlett, R. G. Smith, S. Ho, J. C. Gee, G. Gerig. User-guided 3D active contour segmentation of anatomical structures: Significantly improved efficiency and reliability. *NeuroImage*, vol. 31, no. 3, pp. 1116–1128, 2006. DOI: 10.1016/j.neuroimage.2006.01.015.

[192] A. Fedorov, R. Beichel, J. Kalpathy-Cramer, J. Finet, J. C. Fillion-Robin, S. Pujol, C. Bauer, D. Jennings, F. Fennessy, M. Sonka, J. Buatti, S. Aylward, J. V. Miller, S. Pieper, R. Kikinis. 3D Slicer as an image computing platform for the quantitative imaging network. *Magnetic Resonance Imaging*, vol. 30, no. 9, pp. 1323–1341, 2012. DOI: 10.1016/j.mri.2012.05.001.

[193] D. Mason, scaramallion, mrbean-bremen, rhaxton, J. Suever, Vanessasaurus, D. P. Orfanos, G. Lemaitre, A. Panchal, A. Rothberg, M. D. Herrmann, J. Massich, J. Kerns, K. van Golen, T. Robitaille, S. Biggs, moloney, C. Bridge, M. Shun-Shin, B. Conrad, pawelzajdel, M. Mattes, Y. Lyu, F. C. Morency, T. Cogan, H. Meine, J. Wortmann. pydicom/pydicom: Pydicom 2.3.0: Zenodo, [Online], Available: https://doi.org/10.5281/zenodo.6394735, July 28, 2022.

[194] M. Brett, C. J. Markiewicz, M. Hanke, M. A. Côté, B. Cipollini, P. McCarthy, D. Jarecka, C. P. Cheng, Y. O. Halchenko, M. Cottaar, E. Larson, S. Ghosh, D. Wassermann, S. Gerhard, G. R. Lee, H. T. Wang, E. Kastman, J. Kaczmarzyk, R. Guidotti, J. Daniel, O. Duek, A. Rokem, C. Madison, B. Moloney, F. C. Morency, M. Goncalves, R. Markello, C. Riddell, A. Sólon, C. Burns, J. Millman, A. Gramfort, J. Leppäkangas, J. J. F. van den Bosch, R. D. Vincent, H. Braun, K. Subramaniam, D. Papadopoulos Orfanos, A. Van, K. J. Gorgolewski, P. R. Raamana, J. Klug, B. N. Nichols, E. M. Baker, S. Hayashi, B. Pinsard, C. Haselgrove, M. Hymers, O. Esteban, S. Koudoro, F. Pérez-Garc'ia, J. Dockès, N. N. Oosterhof, B. Amirbekian, I. Nimmo-Smith, L. Nguyen, S. Reddigari, S. St-Jean, E. Panfilov, F. Garyfallidis, G. Varoquaux, J. H. Legarreta, K. S. Hahn, L. Waller, O. P. Hinds, B. Fauber, J. Roberts, J. B. Poline, J. Stutters, K. Jordan, M. Cieslak, M. E. Moreno, T. Hrnčiar, V. Haenel, Y. Schwartz, Z. Baratz, B. C. Darwin, B. Thirion, C. Gauthier, I. Solovey, I. Gonzalez, J. Palasubramaniam, J. Lecher, K. Leinweber, K. Raktivan, M. Calábková, P. Fischer, P. Gervais, S. Gadde, T. Ballinger, T. Roos, V. R. Reddam. nipy/nibabel: Zenodo, [Online], Available: https://doi.org/10.5281/zenodo.6658382, 2022.

[195] B. C. Lowekamp, D. T. Chen, L. Ibáñez, D. Blezek. The design of SimpleITK. *Frontiers in Neuroinformatics*, vol. 7, Article number 45, 2013. DOI: 10.3389/fninf.2013.00045.

[196] G. Bradski. The OpenCV library. *Dr. Dobb's Journal: Software Tools for the Professional Programmer*, vol. 25, no. 11, pp. 120–123, 2000.

[197] P. Virtanen, R. Gommers, T. E. Oliphant, M. Haberland, T. Reddy, D. Cournapeau, E. Burovski, P. Peterson, W. Weckesser, J. Bright, S. J. van der walt, M. Brett, J. Wilson, K. J. Millman, N. Mayorov, A. R. J. Nelson, E. Jones, R. Kern, E. Larson, C. J. Carey, İ. Polat, Y. Feng, E. W. Moore, J. Vanderplas, D. Laxalde, J. Perktold, R. Cimrman, I. Henriksen, E. A. Quintero, C. R. Harris, A. M. Archibald, A. H. Ribeiro, F. Pedregosa, P. van Mulbregt. SciPy 1.0 Contributors. SciPy 1.0: Fundamental algorithms for scientific computing in Python. *Nature Methods*, vol. 17, no. 3, pp. 261–272, 2020. DOI: 10.1038/s41592-019-0686-2.

[198] K. Marstal, F. Berendsen, M. Staring, S. Klein. SimpleElastix: A user-friendly, multi-lingual library for medical image registration. In *Proceedings of IEEE Conference on Computer Vision and Pattern Recognition Workshops*, Las Vegas, USA, pp. 574–582, 2016. DOI: 10.1109/CVPRW.2016.78.

[199] M. P. Heinrich, M. Jenkinson, M. Brady, J. A. Schnabel. MRF-based deformable registration and ventilation estimation of lung CT. *IEEE Transactions on Medical Imaging*, vol. 32, no. 7, pp. 1239–1248, 2013. DOI: 10.1109/TMI.2013.2246577.

[200] F. Pedregosa, G. Varoquaux, A. Gramfort, V. Michel, B. Thirion, O. Grisel, M. Blondel, P. Prettenhofer, R. Weiss, V. Dubourg, J. Vanderplas, A. Passos, D. Cournapeau, M. Brucher, M. Perrot, É. Duchesnay. Scikit-learn: Machine learning in python. *The Journal of Machine Learning Research*, vol. 12, pp. 2825–2830, 2011.

[201] A. Paszke, S. Gross, F. Massa, A. Lerer, J. Bradbury, G. Chanan, T. Killeen, Z. M. Lin, N. Gimelshein, L. Antiga, A. Desmaison, A. Köpf, E. Yang, Z. DeVito, M. Raison, A. Tejani, S. Chilamkurthy, B. Steiner, L. Fang, J. J. Bai, S. Chintala. PyTorch: An imperative style, high-performance deep learning library. In *Proceedings of the 33rd Conference on Neural Information Processing Systems*, Vancouver, Canada, Article No. 721, 2019.

[202] The MONAI Consortium. Project MONAI: Zenodo, [Online], Available: https://doi.org/10.5281/zenodo.4323059, July 28, 2022.

[203] A. Traverso, L. Wee, A. Dekker, R. Gillies. Repeatability and reproducibility of radiomic features: A systematic review. *International Journal of Radiation Oncology · Biology · Physics*, vol. 102, no. 4, pp. 1143–1158, 2018. DOI: 10.1016/j.ijrobp.2018.05.053.

[204] R. Berenguer, M. del Rosario Pastor-Juan, J. Canales-Vázquez, M. Castro-García, M. V. Villas, F. M. Legorburo, S. Sabater. Radiomics of CT features may be nonreproducible and redundant: Influence of CT acquisition parameters. *Radiology*, vol. 288, no. 2, pp. 407–415, 2018. DOI: 10.1148/radiol.2018172361.

[205] M. Meyer, J. Ronald, F. Vernuccio, R. C. Nelson, J. C. Ramirez-Giraldo, J. Solomon, B. N. Patel, E. Samei, D. Marin. Reproducibility of CT radiomic features within the same patient: Influence of radiation dose and CT reconstruction settings. *Radiology*, vol. 293, no. 3, pp. 583–591, 2019. DOI: 10.1148/radiol.2019190928.

[206] S. Zheng, Y. Song, T. Leung, I. Goodfellow. Improving the robustness of deep neural networks via stability training. In *Proceedings of IEEE Conference on Computer Vision and Pattern Recognition*, Las Vegas, USA, pp. 4480–4488, 2016. DOI: 10.1109/CVPR.2016.485.

[207] F. Orlhac, F. Frouin, C. Nioche, N. Ayache, I. Buvat. Validation of a method to compensate multicenter effects affecting CT radiomics. *Radiology*, vol. 291, no. 1, pp. 53–59, 2019. DOI: 10.1148/radiol.2019182023.

[208] A. Zwanenburg, M. Vallières, M. A. Abdalah, H. J. W. L. Aerts, V. Andrearczyk, A. Apte, S. Ashrafinia, S. Bakas, R. J. Beukinga, R. Boellaard, M. Bogowicz, L. Boldrini, I. Buvat, G. J. R. Cook, C. Davatzikos, A. Depeursinge, M. C. Desseroit, N. Dinapoli, C. V. Dinh, S. Echegaray, I. E. Naqa, A. Y. Fedorov, R. Gatta, R. J. Gillies, V. Goh, M. Götz, M. Guckenberger, S. M. Ha, M. Hatt, F. Isensee, P. Lambin, S. Leger, R. T. H. Leijenaar, J. Lenkowicz, F. Lippert, A. Losnegaard, K. H. Maier-Hein, O. Morin, H. Müller, S. Napel, C. Nioche, F. Orlhac, S. Pati, E. A. G. Pfaehler, A. Rahmim, A. U. K. Rao, J. Scherer, M. M. Siddique, N. M. Sijtsema, J. S. Fernandez, E. Spezi, R. J. H. M. Steenbakkers, S. Tanadini-Lang, D. Thorwarth, E. G. C. Troost, T. Upadhaya, V. Valentini, L. V. V. Dijk, J. V. Griethuysen, F. H. P. V. Velden, P. Whybra, C. Richter, S. Löck. The Image biomarker standardization initiative: Standardized quantitative radiomics for high-throughput image-based phenotyping. *Radiology*, vol. 295, no. 2, pp. 328–338, 2020. DOI: 10.1148/radiol.2020191145.

[209] C. Parmar, J. D. Barry, A. Hosny, J. Quackenbush, H. J. W. L. Aerts. Data analysis strategies in medical imaging. *Clinical Cancer Research*, vol. 24, no. 15, pp. 3492–3499, 2018. DOI: 10.1158/1078-0432.CCR-18-0385.

[210] N. Srivastava, G. Hinton, A. Krizhevsky, I. Sutskever, R. Salakhutdinov. Dropout: A simple way to prevent neural networks from overfitting. *Journal of Machine Learning Research*, vol. 15, no. 1, pp. 1929–1958, 2014.

[211] J. Konečný, H. B. McMahan, D. Ramage, P. Richtárik. Federated optimization: Distributed machine learning for on-device intelligence, [Online], Available: http://arxiv.org/abs/1610.02527, March 18, 2022.

[212] Q. Yang, Y. Liu, T. J. Chen, Y. X. Tong. Federated machine learning: Concept and applications. *ACM Transactions on Intelligent Systems and Technology*, vol. 10, no. 2, Article number 12, 2019. DOI: 10.1145/3298981.

[213] J. Pearl. Causal inference. In *Proceedings of Workshop on Causality: Objectives and Assessment*, Whistler, Canada, pp. 39–58, 2010.

[214] D. C. Castro, I. Walker, B. Glocker. Causality matters in medical imaging. *Nature Communications*, vol. 11, no. 1, Article number 3673, 2020. DOI: 10.1038/s41467-020-17478-w.

Jiaqi Li received the B. Eng. degree in automation from Beihang University, China in 2018. He is currently a Ph. D. degree candidate in bioinformatics at Department of Automation, Tsinghua University, China.

His research interests include machine learning and its application for medical image analysis.

E-mail: li-jq18@mails.tsinghua.edu.cn
ORCID iD: 0000-0001-8967-5714

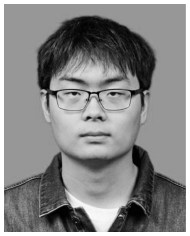

Zhuofeng Li received the B. Eng. degree in automation from Tsinghua University, China in 2018. He is currently a master student in automation, Tsinghua University, China.

His research interests include machine learning and medical image analysis.

E-mail: lzf22@mails.tsinghua.edu.cn

Lei Wei received the B. Eng. and Ph. D. degrees in automation from Tsinghua University, China in 2013 and 2019, respectively. He worked at Department of Automation, Tsinghua University as a postdoctoral fellow from 2019 to 2021, and then joint Beijing National Research Center for Information Science and Technology (BNRIST), Tsinghua University as an assistant research fellow.

His research interests include systems biology, synthetic biology and single-cell bioinformatics.

E-mail: weilei92@tsinghua.edu.cn

ORCID iD: 0000-0002-1546-6458

Xuegong Zhang received the B. Eng. degree in industrial automation and the Ph. D. degree in pattern recognition and intelligent systems from Tsinghua University, China in 1989 and 1994, respectively. He joined Faculty of Department of Automation, Tsinghua University, China in 1994. From 2001 to 2002, he worked at Harvard School of Public Health as a visiting scientist. He is currently a professor of pattern recognition and bioinformatics in Department of Automation, Tsinghua University, and is an adjunct professor in School of Life Sciences and School of Medicine, Tsinghua University. He is the director of Bioinformatics Division, Beijing National Research Center for Information Science and Technology (BNRIST). He was elected as the Fellow of the International Society for Computational Biology (ISCB) and of the Chinese Association of Artificial Intelligence (CAAI) in 2020.

His research interests include machine learning methods and their applications in bioinformatics and medical data analysis, including digital twin systems of life, intelligent health and the informatics architecture of human cellular and molecular portraitures.

E-mail: zhangxg@tsinghua.edu.cn (Corresponding author)

ORCID iD: 0000-0002-9684-5643

Machine Intelligence Research

Citation: J. Li, Z. Li, L. Wei, X. Zhang. Machine learning in lung cancer radiomics. *Machine Inteligence Research*, vol.20, no.6, pp.753–782, 2023. https://doi.org/10.1007/s11633–022–1364–x

Articles may interest you

Machine learning for brain imaging genomics methods: a review. *Machine Intelligence Research*, vol.20, no.1, pp.57-78, 2023.
DOI: 10.1007/s11633-022-1361-0

Machine learning for cataract classification/grading on ophthalmic imaging modalities: a survey. *Machine Intelligence Research*, vol.19, no.3, pp.184-208, 2022.
DOI: 10.1007/s11633-022-1329-0

Application of machine learning for online reputation systems. *Machine Intelligence Research*, vol.18, no.3, pp.492-502, 2021.
DOI: 10.1007/s11633-020-1275-7

Encoding-decoding network with pyramid self-attention module for retinal vessel segmentation. *Machine Intelligence Research*, vol.18, no.6, pp.973-980, 2021.
DOI: 10.1007/s11633-020-1277-0

Federated learning with privacy-preserving and model ip-right-protection. *Machine Intelligence Research*, vol.20, no.1, pp.19-37, 2023.
DOI: 10.1007/s11633-022-1343-2

A weighted average consensus approach for decentralized federated learning. *Machine Intelligence Research*, vol.19, no.4, pp.319-330, 2022.
DOI: 10.1007/s11633-022-1338-z

Swarm intelligence research: from bio-inspired single-population swarm intelligence to human-machine hybrid swarm intelligence. *Machine Intelligence Research*, vol.20, no.1, pp.121-144, 2023.
DOI: 10.1007/s11633-022-1367-7

WeChat: MIR

Twitter: MIR_Journal